Pacific Northwest
NATIONAL LABORATORY

PNNL-38755, Rev. 0
WARM-RPT-001, Rev. 0

FY25 Ion Exchange Processing for the West Area Risk Management (WARM) Project

January 2026

AM Westesen
AA Bachman
K Bhakta
S Cheng
AM Carney
LG El Khoury
J Gacutan
EC Good
C Harabagiu
H Jensen
KE Markham
BD Pierson
RA Peterson
TT Trang-Le

U.S. DEPARTMENT of ENERGY

Prepared for the U.S. Department of Energy
under 4.1.23 DE-AC05-76RL01830

DISCLAIMER

This report was prepared as an account of work sponsored by an agency of the United States Government. Neither the United States Government nor any agency thereof, nor Battelle Memorial Institute, nor any of their employees, **makes any warranty, express or implied, or assumes any legal liability or responsibility for the accuracy, completeness, or usefulness of any information, apparatus, product, or process disclosed, or represents that its use would not infringe privately owned rights**. Reference herein to any specific commercial product, process, or service by trade name, trademark, manufacturer, or otherwise does not necessarily constitute or imply its endorsement, recommendation, or favoring by the United States Government or any agency thereof, or Battelle Memorial Institute. The views and opinions of authors expressed herein do not necessarily state or reflect those of the United States Government or any agency thereof.

PACIFIC NORTHWEST NATIONAL LABORATORY
operated by
BATTELLE
for the
UNITED STATES DEPARTMENT OF ENERGY
under Contract DE-AC05-76RL01830

Printed in the United States of America

Available to DOE and DOE contractors from the Office of Scientific and Technical Information,
P.O. Box 62, Oak Ridge, TN 37831-0062
www.osti.gov
ph: (865) 576-8401
fax: (865) 576-5728
email: reports@osti.gov

Available to the public from the National Technical Information Service
5301 Shawnee Rd., Alexandria, VA 22312
ph: (800) 553-NTIS (6847)
or (703) 605-6000
email: info@ntis.gov
Online ordering: http://www.ntis.gov

PNNL-38755, Rev. 0
WARM-RPT-001, Rev. 0

FY25 Ion Exchange Processing for the West Area Risk Management (WARM) Project

January 2026

AM Westesen
AA Bachman
K Bhakta
S Cheng
AM Carney
LG El Khoury
J Gacutan
EC Good
C Harabagiu
H Jensen
KE Markham
BD Pierson
RA Peterson
TT Trang-Le

Prepared for
the U.S. Department of Energy
under Contract DE-AC05-76RL01830

Pacific Northwest National Laboratory
Richland, Washington 99354

Summary

The West Area Risk Management (WARM) Project was established to enable near-term retrieval and pretreatment of tank waste from Hanford's 200 West Area (200W) and to support deployment of an ion exchange (IX) system capable of producing cesium-depleted supernate suitable for offsite treatment and disposal. The WARM experimental campaign was designed to provide key data for design and operational planning of the 200W IX system, which plans to use crystalline silicotitanate (CST) as the active media for cesium removal.

This report documents a comprehensive FY25 experimental campaign designed to produce key technical data required for design and operational planning of the WARM IX system. Testing includes assessing Cs and Sr breakthrough performance in a 4-column system, Cs capacity batch contact testing, phosphate precipitation assessments, reduced-hydroxide feed displacement evaluation, and Sr speciation impacts on Sr removal.

The experimental results provide detailed trends in Cs and Sr loading behavior, breakthrough performance across a 4-column staged IX system, distribution profiles within CST beds, and projections of operational flowrates relative to waste acceptance criteria limits. Table S.1 and Figure S.1 summarize the observed column performance and relevant Cs and Sr loading characteristics.

Table S.1. WARM S1 Simulant Column Performance Summary with CST

Column	WAC Limit Breakthrough (BVs)	50% Cs Breakthrough (BVs)	^{137}Cs Loaded (µCi)	Cs Loaded (mmoles Cs/g CST)	^{90}Sr Loaded (µCi)	Sr Loaded (mmoles Cs/g CST)
Column A	178	1127	1.35E+02	3.71E-02	4.28E+02	6.93E-03
Column B	757	2254	8.07E+01	2.22E-02	4.52E+01	4.83E-04
Column C	1472	3380[(a)]	2.20E+01	6.05E-03	1.15E+01	1.23E-04
Column D	2179	NA	1.38E+00	3.79E-04	8.76E-01	9.36E-06

(a) Extrapolated value
BV = bed volume, 6.0 mL
(b) The time-weighted average flowrate was 1.40 BV/h.

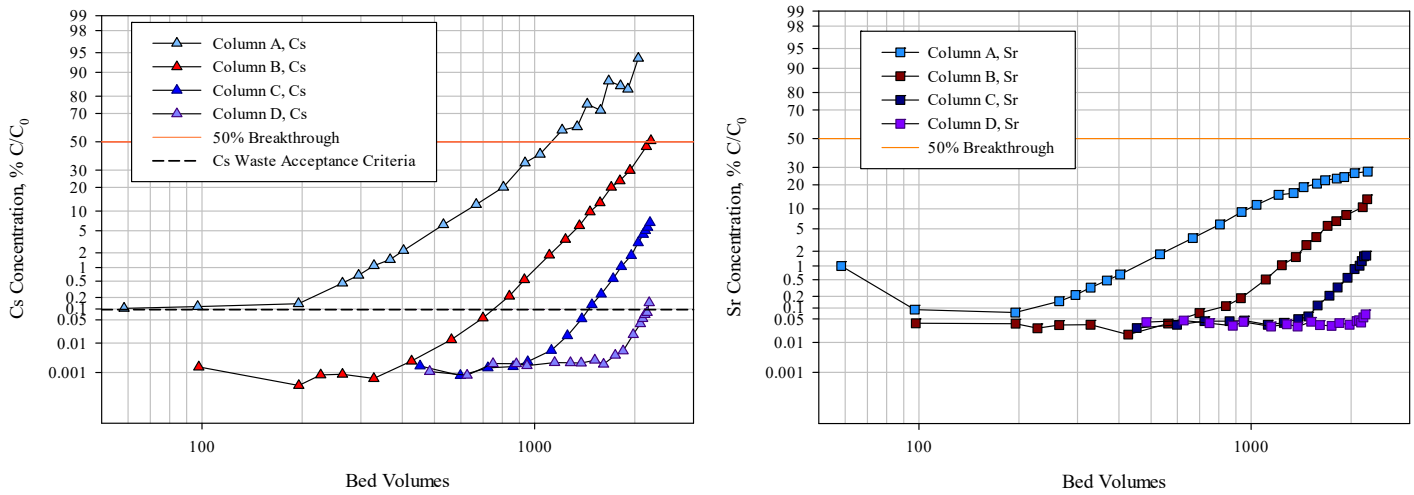

Figure S.1. Column A, B, C, and D Load Profiles for Cs (left) and Sr (right)

Batch contact testing established equilibrium partitioning behavior for the S1–S5 simulants and characterized the influence of matrix chemistry on Cs sorption onto CST. Further evaluations on waste matrix as it pertains to precipitation potential were also conducted. Collectively, these datasets support engineering design choices for WARM system throughput and pretreatment planning.

Acknowledgements

The authors thank Hanford Tank Waste Operations & Closure for funding this work. We also thank the Analytical Support Operations staff Truc Trang-Le, Steven Baum, Leah Arrigo, Christian Perez, and Dave Blanchard for the sample analysis, data processing, and reporting. The authors thank Heather Colburn, Susan Asmussen, and Alfredo Scigliani, and Renee Russell for conducting the technical reviews of the calculation files and this report. The authors also thank David MacPherson and Alyssa Petersen for the quality review of the calculation files, data packages, task instructions and of this report as well as Matt Wilburn for his technical editing contribution to this report.

Acronyms and Abbreviations

200W	200 West Area
BV	bed volume
CST	crystalline silicotitanate
DI	deionized
DOE	U.S. Department of Energy
erf	error function
FD	feed displacement
H2C	Hanford Tank Waste Operations & Closure
IC	ion chromatography
ICP-OES	inductively coupled plasma optical emission spectroscopy
IX	ion exchange
LSC	liquid scintillation counting
NA	not applicable
NQAP	Nuclear Quality Assurance Program
PNNL	Pacific Northwest National Laboratory
SV	system volume
TSCR	Tank Side Cesium Removal
WAC	waste acceptance criteria
WARM	West Area Risk Management
XRD	X-ray diffraction

Contents

Figures

Tables

1.0 Introduction

The West Area Risk Management (WARM) project was created to help enable near-term retrievals of tank waste in the 200 West Area (200W) of the Hanford Site. The U.S. Department of Energy (DOE) and its contractor Hanford Tank Waste Operations & Closure (H2C) are planning to pretreat the tank waste – specifically by removing high-risk radionuclides such as cesium (Cs) and strontium (Sr) – and subsequently immobilize the waste for offsite disposal and storage.

Tank waste supernate will be pretreated by filtering the waste using a Mott Media grade 5 filter and then removing Cs and Sr through ion exchange (IX) columns containing crystalline silicotitanate (CST). The CST beds are expected to be ~157 gallons and will consist of four IXC-150 IX columns operated in series (1-2-3-4). After the Cs breakthrough criteria is met on the fourth column (<0.106 μCi ^{137}Cs/mL for rail transportation and 0.125 μCi ^{137}Cs/mL for truck transportation),[1] the first and second columns will be removed and placed on a storage pad. Two new columns (5 and 6) will then be installed in the processing system and operations will then be restarted with waste flowing through the columns in the order of position 3-4-5-6. The process of changing two columns each time and placing the new columns at the end of the series is performed to increase efficiency for both operations and media use.

Previous support for WARM flowsheet planning developed five simulant formulations appropriate for the tanks under consideration for the 200W preliminary flowsheet (Schonewill et al. 2024). The simulants were formulated to reflect what the potential qualified feed streams to the 200W process modules could look like as single-shell tanks are being retrieved. This report describes testing conducted in support of WARM flowsheet planning and development by assessing Cs and Sr removal performance using CST with five West Area waste simulants (S1-S5). Specific objectives of the current study were as follows:

1. Conduct a 4-column system operated in series and assess Cs and Sr breakthrough performance using the S1 simulant at ambient temperature (~20 °C). Process feed until the Cs breakthrough criteria is met on the fourth column.
2. Gamma scan IX columns post processing to determine Cs and Sr load profiles down the length of each column. Reinstall gamma-scanned columns and continue feed processing to determine potential loss of capacity due to column drying.
3. Perform batch contact testing with CST at 20 and 35 °C to determine the Cs load capacity of S1- S5 simulants and the compositional and temperature impacts on removal.
4. Determine PO_4 precipitation conditions at 16 °C with the S4 simulant at 0.06 (native), 0.1, and 0.2 M PO_4. Assess potential plugging impacts in a flowthrough column configuration.
5. Assess potential aluminum (Al) precipitation with a reduced hydroxide feed displacement (FD) solution at 13 and 25 °C. FD solutions tested include 0.1 M NaOH (standard), 0.01 M NaOH, deionized (DI) water, and Columbia River water.
6. Evaluate the effect of Sr speciation on Sr removal by CST at ambient temperature (21 °C). Conduct batch contact tests using simple simulant matrices containing varying concentrations of NaOH, $NaNO_3$, $NaNO_2$, and Na_2CO_3 to produce different Sr speciation conditions and assess equilibrium performance across four Sr concentrations.

H2C funded Pacific Northwest National Laboratory (PNNL) to conduct this testing under the statement of work *Ion Exchange Testing for the WARM Project,* Rev. 0, Requisition 377642, dated October 23, 2024. There are no deviations from the statement of work.

[1] RPP-RPT-65461, Rev. 0. 2025. *Dose Rate Scoping Assessment for Potential West Area Tank Treatment Packages using Microshield ®*. Hanford Tank Waste Operations & Closure, LLC. Richland, WA.

2.0 Quality Assurance

This work was conducted with funding from H2C under requisition 377642, *Ion Exchange Testing for the WARM*. This work was performed in accordance with the PNNL Nuclear Quality Assurance Program (NQAP). The NQAP complies with DOE Order 414.1D, *Quality Assurance*, and 10 CFR 830, Subpart A, *Quality Assurance Requirements*. The NQAP uses NQA-1-2012, *Quality Assurance Requirements for Nuclear Facility Applications*, as its consensus standard and NQA-1-2012, Subpart 4.2.1, as the basis for its graded approach to quality. The data associated with this report was collected under technology readiness level 5, the highest level of applied research under NQAP.

3.0 Test Conditions

This section describes the CST media, S1-S5 simulants, column and batch contact IX conditions, precipitation and FD assessments, and all associated sample analysis. All testing was conducted in accordance with a task plan prepared by PNNL and approved by H2C.[2]

3.1 CST Media

The CST used in this testing was procured by H2C under the previous contractor name Washington River Protection Solutions in ten 5-gallon buckets (149 kg total) of IONSIV R9140-B,[3] lot number 2002009604, from Honeywell UOP, LLC. The CST was transferred to PNNL for use in laboratory testing described herein. Details of the procurement and material properties can be found elsewhere (Fiskum et al. 2019). Before using in-column and batch contact testing, the CST was sieved to <30 mesh and pretreated by contacting with 0.1 M NaOH successively until fines were no longer observed. The <30-mesh CST sieve cut has been shown to provide appropriate performance scaling to a full-height Tank Side Cesium Removal (TSCR) column (Westesen et al. 2020).

3.2 WARM Simulants S1–S5

PNNL contracted the production of 300 gallons of S1, S2, S3, S4, and S5 simulants to Noah Technologies, Inc. (San Antonio, Texas). The simulant preparations were conducted as defined by Schonewill et al. (2024), with target component concentrations provided in Table 3.1. The reagents used to make the simulants were assayed at 99.2% or better. However, the sheer scale of the production process required very large quantities of salts to be used, and a small metal impurity fraction could result in kilogram quantities of insoluble metal hydroxides.

Sixteen liters of the S1 and two liters each of the S2-S5 300-gallon batches were subsampled to support the IX testing reported herein. The remaining simulant was used in filtration testing covered in a separate report (Schonewill et al. 2025).

A suite of analyses consisting of density, anions, metal concentrations, and Cs and Sr was conducted on aliquots of the simulant samples upon arrival at PNNL. Analysis results agreed with the preparation formulation within a relative 7%. The solution densities were measured in a volumetric flask at 1.24, 1.24, 1.09, 1.17, and 1.18 g/mL for the S1 through S5 solutions, respectively. The simulant preparations were considered accurate.

[2] Westesen, A. M. 2025. *FY25 Ion Exchange Processing for the West Area Risk Management (WARM) Project.* Pacific Northwest National Laboratory, Task Plan WARM-TP-001, Rev. 0.0. Richland, WA. Not publicly available.

[3] R9140-B is provided in the sodium form by the vendor.

Table 3.1. S1 through S5 Simulant Target Compositions

Component	S1 Target Conc. (M)	S2 Target Conc. (M)	S3 Target Conc. (M)	S4 Target Conc. (M)	S5 Target Conc. (M)
$Al(NO_3)_3 \cdot 9H_2O$	0.17	0.05	0.03	0.07	0.07
$CsNO_3$	2.77E-05	6.16E-06	5.13E-06	9.24E-06	8.72E-06
$Sr(NO_3)_2$	3.31E-06	3.78E-06	3.31E-06	3.78E-06	8.03E-06
$Na_2Cr_2O_7 \cdot 2H_2O$	1.85E-03	2.38E-03	9.40E-04	2.05E-03	7.99E-03
50% (w/w) NaOH solution	2.10	0.67	0.41	1.08	1.09
$Na_3PO_4 \cdot 12H_2O$	0.05	0.05	0.04	0.06	0.04
KNO_3	0.04	0.01	0.01	0.02	0.01
NaCl	0.11	0.03	0.02	0.04	0.04
$CaCl_2 \cdot 2H_2O$	7.07E-04	6.33E-04	6.87E-04	2.12E-03	2.11E-04
NaF	0.01	0.01	0.02	0.02	0.02
Na_2SO_4	0.04	0.04	0.02	0.04	0.05
$NaCH_3CO_2$	0.03	0.00	0.01	0.01	--
$NaCHO_2$	0.03	0.00	0.01	0.01	--
$Na_2C_2O_4$	0.01	0.02	0.01	0.02	0.02
$NaNO_2$	1.13	0.25	0.22	0.41	0.36
$NaNO_3$	1.08	3.49	0.75	1.29	1.87
$Na_2CO_3 \cdot H_2O$	0.44	0.17	0.12	0.20	0.22
Total Na	**5.63**	**5.04**	**1.90**	**3.56**	**4.11**

3.3 4-Column Ion Exchange Processing

This section describes the process conditions of the IX column system used for S1 simulant testing. The preparations and column testing were conducted in accordance with a PNNL task instruction.[4]

3.3.1 Ion Exchange Column System

Figure 3.1 illustrates the IX system configuration used for column testing with the S1 simulant. Each column contained 6.0 mL of pretreated (<30 mesh, 0.1 M NaOH rinsed) CST, supported by a 200-mesh stainless-steel screen welded to an O-ring. A bed of 4-mm glass beads minimized the void volume below the media, and a graduated centimeter scale was affixed for visual bed-height monitoring.

The valve manifold included four Swagelok valves used to collect effluent from the lead (column A), middle (column B), first polish (column C), and second polish (column D) columns, respectively.

[4] Westesen, A. M. 2025. *4-Column WARM Simulant S1 Crystalline Silicotitanate Ion Exchange (IX) Testing.* Pacific Northwest National Laboratory, Task Instruction WARM-TI-002. Richland, WA. Implemented May 2025. Not publicly available.

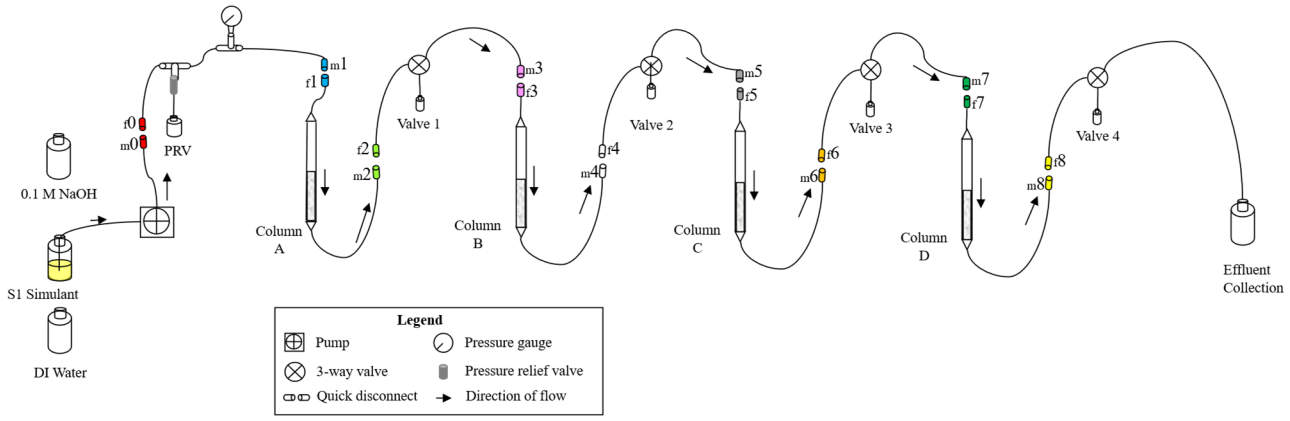

Figure 3.1. Schematic of the S1 Simulant Column System

3.3.2 S1 Column Ion Exchange Process Conditions

Once the IX columns were installed, system integrity was verified and pump calibration was performed using 0.1 M NaOH. The flowrate was controlled with a remotely operated Fluid Metering, Inc. manufactured stroke-rate controller. With additional adjustment of the stroke length, the pump could deliver flowrates from 0.1 to ~15 mL/min. The actual volume pumped was determined using the mass of the fluid collected divided by the fluid density. Flowrate was determined from the calculated volume processed divided by the collection time.

Before processing through the columns, a 15-L S1 simulant container was spiked with ^{137}Cs, ^{85}Sr, and ^{90}Sr tracer solutions sufficient to provide measurable decontamination factors when measured by gamma spectroscopy for the ^{137}Cs and ^{85}Sr and beta counting for ^{90}Sr. The tracers were added to the simulant by volumetric pipette directly into the simulant container. The tracers were mixed into the simulant to create a homogenous distribution and allowed to equilibrate overnight in the solution. Figure 3.2 is a photograph of the system and column assembly as used in the fume hood.

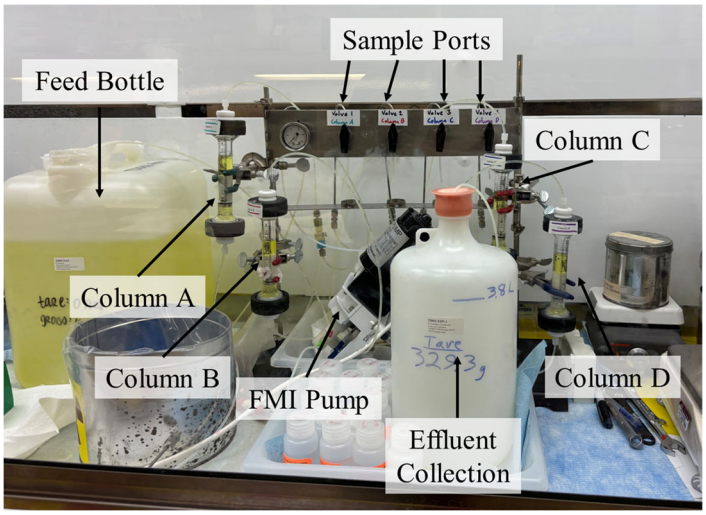

Figure 3.2. Ion Exchange Column Apparatus in the Fume Hood

The flowrate through the system was specifically chosen to bound potential WARM operations between 3.5 and 7.5 gpm when normalized for column throughput. This resulted in a residence time of 1.4 bed volumes (BVs) per hour through the system. The specific processing parameters achieved for the testing are presented in Table 3.2.

Table 3.2. Experimental Conditions for S1 Column Processing at 20 °C, June 10 through August 16, 2025

		Volume		Flowrate		Duration
Process Step	Solution	(BV)	(mL)	(BV/h)	(mL/min)	(h)
Loading column A	S1 Simulant	2242	13453	1.40	0.140	1607:23
Loading column B[(a)]	S1 Simulant	2234	13405	1.40	0.140	1607:23
Loading column C[(a)]	S1 Simulant	2220	13318	1.40	0.140	1607:23
Loading column D[(a)]	S1 Simulant	2210	13261	1.40	0.140	1607:23
Feed displacement	0.1 M NaOH	12.8	76.7	3.13	0.313	4:05
Water rinse	DI water	12.2	73.0	3.04	0.304	4:00
Flush with compressed air	NA	10.9	65.3	NA	NA	NA

(a) The feed volume through columns B, C, and D was reduced relative to that of the preceding column because samples collected from the preceding columns did not enter the subsequent column.
BV = bed volume (6.0 mL as measured in graduated cylinder); NA = not applicable.

The total cumulative S1 simulant volume processed was 13.2 L (2200 BVs). The process cycle mimicked, as best as possible, the planned process flow anticipated for WARM in terms of potential BV/h (i.e., contact time), FD, and water rinse. It was understood that the feed linear flow superficial velocity in this small-column configuration (0.14 cm/min) could not begin to match that of the full-height processing configuration, but the objective was to match contact time in the bed.

During the loading phase, nominal 2-mL samples were collected from columns A, B, C, and D at the sample collection ports (see Figure 3.1, valves 1, 2, 3, and 4). Sampling from the columns necessitated brief (~10-min) interruptions of flow to the downstream columns. Samples were collected after the first 60 BVs were processed and again at nominally 30- to 150-BV increments.

The FD effluent was collected in bulk in a 125-mL polyethylene bottle. The water rinse was similarly collected. The fluid-filled volume was expelled with compressed air in ~4 min. The collected volume (~65 mL) did include the interstitial fluid space between the CST beads but was not expected to include fluid in the CST pore space. Hours of additional gas flow were required to dry the CST enough to be free flowing. Post column drying, columns were gamma-scanned to assess Cs and Sr breakthrough profiles down the length of each column. At the conclusion of gamma scanning, columns were reinstalled in the system and another ~100 BVs of feed was processed to determine loss of Cs capacity, if any, that occurred after column drying.

3.3.3 Column Gamma Scanning

Each of the four IX columns from the S1 simulant processing were scanned to assess the overall nature of the Cs and Sr loading onto the CST. The column measurements were conducted using a customized detection system incorporating a Mirion high-purity germanium detector surrounded by lead shielding. The detector was shielded with lead bricks to prevent radiation streaming from the column and the general laboratory background. The entire setup was assembled on a CE Mobile Lift Table with a 1000-kg capacity. Figure 3.3 shows the entire system with the detector and collimator assembly in the high position (left) along with a close-up view of the column holder.

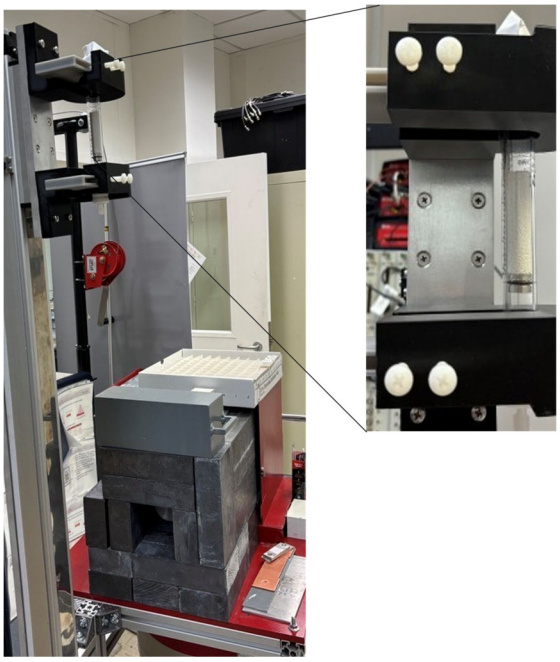

Figure 3.3. ^{137}Cs and ^{85}Sr Column Scanning System

The opening in the lead shielding contained a lead collimator that provided a ~0.1-in. horizontal opening (not pictured) so that the columns could be measured in small segments. The stepper motor controlling the column movement was calibrated and set to move in 0.1-in. steps for each scan. The detector parameters, data acquisition, and scanning algorithm were performed on a Windows 11 computer running the Mirion Genie2000 gamma spectroscopy suite (v3.4). A Windows PowerShell script was used to control both the movement of the columns on the track and the collection of gamma data from the detector.

Energy and efficiency calibrations were performed by taping two button sources with known activities on the bottom of the last column measured (column D). Because the entire column was scanned, there was some distance between the sources and the contents of the column that were being scanned due to its geometry, so the sources did not interfere with any quantification. The ^{133}Ba source was 3.807 MBq on 15 March 2016 with serial number 1868-19-1 and the ^{137}Cs source was 3.707 MBq on 15 March 2016 with serial number 1868-19-3. The ^{133}Ba 356-keV line and ^{137}Cs 661.7-keV line were used as calibration points. To find the efficiency at the ^{85}Sr 514-keV line, a linear fit was made in log-log space between the 356 and 661.7 keV lines using the equation $Efficiency = 6.45283E\text{-}03*Energy^{-8.02743E\text{-}01}$. The measurement of these sources also verified that the collimator provided a limited field of view for detection and not a cone-shaped larger field.

Data were acquired and spectra saved at each position along the length of the column in 0.1-in. steps, with each count being 1000 seconds long. Each measurement point's spectrum was analyzed in Genie2000 to find the quantifiable activity from the energy and efficiency calibration described above. ^{85}Sr was quantified using its 514-keV gamma and ^{137}Cs was quantified using its 661.7-keV gamma. A peak fit from one measurement point in the first measured column (with the strongest activities) was propagated to all other spectra to avoid variations in activity from analyst bias.

3.4 S1- S5 Cs Batch Contact Conditions

Batch contact experiments with each of the five WARM simulants were conducted to evaluate Cs loading in each of the matrices at 20 and 35 °C. The batch contact processing activities were conducted according to a task instruction (internally prepared and reviewed).[5]

The Cs concentration in each of the simulants was increased to 20, 60, 200, and 2000 mg/L using stock solutions of 0.75 and 0.084 M $CsNO_3$. The stock solutions of cesium nitrate were prepared volumetrically by dissolving reagent-grade $CsNO_3$ in DI water. Calculated volumes of the Cs stock solutions were delivered to polyethylene bottles containing each of the simulants, and the mass of the spike was measured. Solutions were prepared gravimetrically, and exact volumes were calculated from mass and density measurements. A ^{137}Cs tracer was also added to each simulant, resulting in a nominal ^{137}Cs concentration of 0.11 µCi/mL. The simulants were equilibrated (overnight) with the stable Cs and tracer ^{137}Cs. A 2-mL subsample from each mixture was collected and served to provide the initial ^{137}Cs concentration (C_0) measurement.

Approximately 0.075 g (dry mass basis) of CST was measured into 20-mL vials for each simulant test. The dry mass of the exchanger was verified using an F-factor determined at 105 °C, with F-factor samples collected before and after each batch contact series. Aliquots (15-mL) of each simulant spiked with Cs stock solution and ^{137}Cs were added to the appropriate vials (in duplicate) and the exact solution volume transferred was calculated from net solution mass and density. The typical solution-to-mass ratio was maintained near 200 mL/g to ensure near-equilibrium conditions.

Batch contacts were conducted at both 25 and 35 °C to determine temperature impacts on overall Cs removal. Because of simulant delivery timing, the S1 and S3 batch contact tests were carried out at the same time, and the S2, S4, and S5 tests were conducted together in a separate set. Figure 3.4 shows the resulting temperature fluctuations for each set of tests, with error bars representative of the 2.2 °C measurement uncertainty of a Type K thermocouple. Table 3.3 presents the weighted mean temperature for each set of batch contacts.

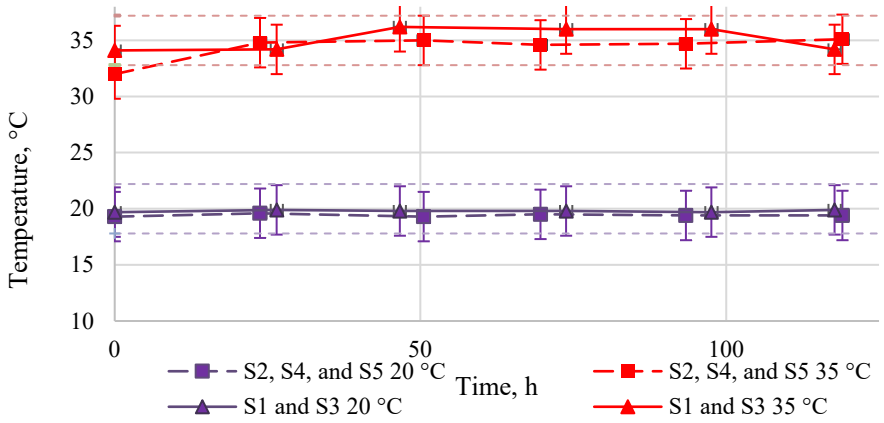

Figure 3.4. Temperature Profiles of Batch Contact Testing with S1-S5 WARM Simulants

[5] Westesen A. M. 2025. *Isotherm Batch Contact Testing of Cs onto Crystalline Silicotitanate in S1 – S5 WARM Simulants.* Pacific Northwest National Laboratory, Task Instruction WARM-TI-004. Richland, WA. Implemented June 2025. Not publicly available.

Table 3.3. Average Contact Temperature

Simulant Test	Target Temperature (°C)	Weighted Mean Temperature (°C)
S1 and S3	20	19.8
S2, S4, and S5	20	19.4
S1 and S3	35	35.3
S2, S4, and S5	35	34.5

After contact, 2 mL of the simulant was removed and filtered through a 0.45-micron pore size nylon syringe filter and transferred to a glass vial for gamma energy analysis. The ^{137}Cs activity measured by gamma energy analysis in pre- and post-contacted solutions was used to determine the total Cs exchange. Analysis and data reduction were conducted using the methods previously reported (Fiskum et al. 2019). The isotherm data were fitted to a Freundlich/Langmuir hybrid equilibrium fit (Hamm et al. 2002).

The batch distribution coefficients were calculated according to Eq (3.1):

$$\frac{(A_0 - A_1)}{A_1} \times \frac{V}{M \times F} = K_d \tag{3.1}$$

where:

A_0 = initial ^{137}Cs concentration (µCi/mL)
A_1 = final (equilibrium) ^{137}Cs concentration (µCi/mL)
V = volume of the batch contact liquid (mL)
M = measured mass of CST (g)
F = F-factor, mass of the 105 °C dried CST divided by the mass of the undried CST
K_d = batch-distribution coefficient (mL/g)

Final (equilibrium) Cs concentrations (C_{Eq}) were calculated relative to the tracer recovered in the contacted samples (A_1) and the initial metal concentration (C_0) according to Eq. (3.2):

$$C_0 \times \left(\frac{A_1}{A_0}\right) = C_{Eq} \tag{3.2}$$

where:

C_0 = initial Cs concentration in solution (µg/mL or M)
C_{Eq} = equilibrium Cs concentration in solution (µg/mL or M)

The equilibrium Cs concentrations loaded onto the CST (Q in units of mmoles Cs per gram of dry CST mass) were calculated according to Eq. (3.3):

$$\frac{C_0 \times V \times \left(1 - \frac{A_1}{A_0}\right)}{M \times F \times 1000 \times FW} = Q \tag{3.3}$$

where:

Q = equilibrium Cs concentration in the CST (mmole/g CST)
1000 = conversion factor to convert µg to mg
FW = Cs formula weight

3.5 Phosphate Precipitation Assessment with S4 Simulant

The potential for phosphate (PO_4^{3-}) precipitation was evaluated at 16 °C with the S4 simulant to define the upper PO_4 concentration limit that can be stably maintained under WARM IX processing conditions. The S4 simulant was selected from the five WARM simulants available because it had the highest native PO_4 concentration at 0.06 M. This simulant was tested as-is and at adjusted PO_4 concentrations of 0.1 and 0.2 M. All precipitation activities were conducted according to a task instruction (internally prepared and reviewed).[6]

Three 100-mL aliquots of the S4 simulant were dispensed into volumetric flasks and assigned phosphate concentration targets of 0.0637 M (native control), 0.10 M, and 0.20 M. For the 0.1 and 0.2 M PO_4 conditions, phosphate was introduced using trisodium phosphate dodecahydrate ($Na_3PO_4 \cdot 12H_2O$). The required $Na_3PO_4 \cdot 12H_2O$ mass additions were calculated using Eq. (3.4):

$$\mathrm{M_{s,g}} = (C_{goal} - 0.0637)\frac{v}{2.6307} \tag{3.4}$$

where C_{goal} is the desired phosphate molarity and v is the sample volume (100 mL). Salt additions were weighed to within ± 1 % of target mass and dissolved directly into the simulant while stirring. Each solution was heated to 60 °C with magnetic stirring to ensure complete phosphate dissolution, then cooled to ambient temperature. Samples were equilibrated for 24 h at room temperature and then filtered to remove any precipitation that occurred. Filtered aliquots (0.45-µm filter pore size) were collected, in duplicate, for initial phosphate concentration analysis by ion chromatography (IC) and inductively coupled plasma optical emission spectroscopy (ICP-OES).

Following initial sampling, the sealed bottles were placed in a temperature-controlled chamber maintained at 16 ± 2.2 °C, representative of lower bound tank waste supernate temperature conditions. A reference bottle filled with DI water was equipped with a thermocouple that verified temperature stability. Samples were held at this temperature for 72 h to allow any potential PO_4 precipitation to equilibrate. After the contacts were completed, filtered liquid samples from the post-cooling bottles were subsampled, in duplicate, and submitted for IC and ICP-OES quantification of phosphate and major cations/anions. Collected solid precipitant, if found, was analyzed by Radiochemical Processing Laboratory Analytical Support Operations via X-ray diffraction (XRD). The extent of phosphate precipitation was determined from the difference between pre- and post-cooling dissolved phosphate concentrations.

Conditions from the batch assessment drove a column evaluation using the S4 simulant at its native 0.06 M PO_4 concentration. The simulant was passed through a single column filled with 10 mL of CST at a nominal 1.9 BV/h flowrate at 16 °C. Pressure in the system was monitored for 1 week to determine if a flowthrough system propagated a nucleation site for PO_4 precipitation, and if so, what the downstream pressure and plugging effects were.

[6] El Khoury, L. 2025. *Determining the solubility of phosphate ions in WARM S4.* Pacific Northwest National Laboratory, Task Instruction WARM-TI-005. Richland, WA. Implemented June 2025. Not publicly available.

3.6 Reduced Feed Displacement Concentration Assessment

A reduced hydroxide FD was evaluated at 13 and 25 °C to determine the potential for aluminum precipitation when contacted with displacement solutions containing less than 0.1 M NaOH. The current use of 0.1 M NaOH comes from the potential for aluminum in the waste streams to precipitate as $Al(OH)_3$ upon conversion from the strong base to water. The S1 simulant was used as the feed for the assessment as it contained the highest aluminum concentration among the five WARM simulants at 0.17 M, making it the most sensitive matrix for evaluating hydroxide-driven precipitation. All precipitation activities followed a task instruction (internally prepared and reviewed).[7]

Reagent preparation used American Chemical Society reagent-grade chemicals. Sodium hydroxide solutions were prepared gravimetrically at target molarities of 0.1 and 0.01 M NaOH. Additional displacement solutions included DI water and Columbia River water to represent potential low-alkalinity displacement streams.

Aliquots (nominal 50 mL) of S1 simulant were prepared in polypropylene vials for each FD condition, in duplicate. Conditions were assessed both with and without CST solids present to evaluate potential sorbent-mediated precipitation. The CST used in this testing was a subsample of the pretreated CST discussed in Section 3.4. Temperature control at 13 °C was achieved using a refrigerated environmental chamber. Ambient (25 °C) tests were conducted under general laboratory conditions (20 to 25 °C). Samples were allowed to equilibrate for a minimum of 25 days for the 25 °C series and 13 days for the chilled series. Once equilibrated, samples were contacted with each displacement solution (also set to the designed test temperature) under quiescent conditions. Vials were visually inspected for signs of turbidity or solids formation following the FD addition. Photographs were taken to document sample clarity, color, and precipitate morphology for all test combinations.

Conditions from the batch assessment drove a column evaluation using the S1 simulant and displacing with Columbia River water at 13 °C. The simulant was initially passed through a single column filled with 10 mL of CST at a nominal 1.9-BV/h flowrate. Once the solution filled the column system, 500 mL of Columbia River water was introduced to displace the feed. Pressure in the system was monitored for the duration of the displacement (~24 h) and the system was visually inspected to identify any aluminate precipitation.

3.7 Simple Simulant Sr Speciation Batch Contacts

Eight simple simulants were formulated to enable controlled variation of anions that govern aqueous Sr speciation in Hanford supernates. Sets of matrices were created by independently varying OH, NO_3, NO_2, and CO_3 to a total Na concentration of 5.5 M Na, representative of potential WARM IX feeds. Varying the anion concentrations allowed for multiple Sr-speciation regimes (e.g., hydroxide, nitrate/nitrite, and carbonate complexation domains) to be generated and assessed for overall Sr removal by CST. The Sr simple simulant batch contact activities were conducted according to a task instruction (internally prepared and reviewed).[8]

[7] Colburn, H. A. 2025. *Testing Impact of Feed Displacement Hydroxide Concentration on Aluminum Solubility.* Pacific Northwest National Laboratory, Task Instruction WARM-TI-006. Richland, WA. Implemented July 2025. Not publicly available.

[8] Colburn, H. A. 2025. *Strontium Anion Effects Batch Contacts Testing.* Pacific Northwest National Laboratory, Task Instruction WARM-TI-008. Richland, WA. Implemented August 2025. Not publicly available.

Table 3.4 presents the compositions of the five simple simulants. The batch contact experiments used a ^{90}Sr radiotracer, which has a 0.546 MeV β decay. The method of detection for ^{90}Sr used liquid scintillation counting (LSC), which was achievable in this simulant matrix because no other α or β emitters were present.

Table 3.4. Simple Simulant Composition

Simulant	NaOH (M)	$NaNO_3$ (M)	Na_2CO_3 (M)	$NaNO_2$ (M)
1A	1.0	4.5	–	–
1B	4.5	1.0	–	–
1C	1.0	4.0	0.25	–
1D	1.0	2.8	0.85	–
2A	1.0	–	–	4.5
2B	4.5	–	–	1.0
2C	1.0	–	0.25	4.0
2D	1.0	–	0.85	2.8

CST from lot 2002009604 (Honeywell UOP, LLC product IONSIV R9140-B) was passed through a 30-mesh sieve. The CST was pretreated with 0.1 M NaOH and allowed to air dry until free flowing. An F-factor was determined to account for water content in the CST by drying ~0.3 g of CST at ~105 °C.

Due to limited solubility of Sr in the presence of anions such as CO_3^{2-}, the batch contact methodology typically used for Cs removal was modified to change the solution-to-mass ratio instead of initial Sr concentration in order to change the moles of Sr in solution. A 1.0E-5 M Sr solution was prepared from a 5.5 mM $Sr(NO_3)_2$ solution (in DI water) and spiked with ^{90}Sr. Aliquots of the CST were weighed, and solution volumes were added to target solution-to-mass ratios of 200, 600, 1200, and 2000. The F-factor for the Sr batch contact simulant series was calculated to be 0.932. Samples were conducted, in duplicate, at ambient temperature conditions (~20 °C) with shaking on a Benchmark Incu-Shaker 10LR orbital shaker set to 200 rpm. After the contact period (120 h, as determined from previous kinetic experiments in simple 4.6 M $NaNO_3$/1 M NaOH simulant; Fiskum et al. 2020) was completed, a 200-µL aliquot of the decontaminated supernate was added to a 20-mL LSC cocktail. The samples were shaken to disperse the liquid and counted immediately by LSC beta counting. The ^{90}Sr activity was measured in each of the feed solutions and compared to the post-contact solutions to determine overall Sr removal by CST using Eqs. (3.1) through (3.3). Additionally, electrospray ionization mass spectrometry spectra were collected in an effort to identify the Sr complexes, but the effort was unsuccessful due to the overwhelming amount of Na in solution.

4.0 Results

This section discusses the WARM IX results during column, batch contact, and precipitation testing.

4.1 4-Column Cs and Sr Ion Exchange Processing

The Cs and Sr load behaviors were evaluated with the S1 WARM simulant at ambient temperature. This section discusses load, FD, water rinse, mass balance results, and column gamma scanning for the executed test.

4.1.1 Cs and Sr Loading Results

The S1 simulant was processed at nominally 1.40 BV/h through the 4-column system. Figure 4.1 and Figure 4.2 show the Cs and Sr load profiles for each column on a probability-log scale plot, respectively. In both plots, the x-axis shows the BVs processed and the y-axis shows the effluent Cs or Sr concentration (C) relative to the feed concentration (C_0) in terms of %C/C_0. Feed was processed through the 4-column system for 2200 BVs, at which time the fourth column effluent had reached the waste acceptance criteria (WAC) limit for Cs and testing was concluded. The plots include the 50% C/C_0 indication line in orange and the Cs plot shows the WAC limit, set at 0.0964% C/C_0 (dashed black line).[9]

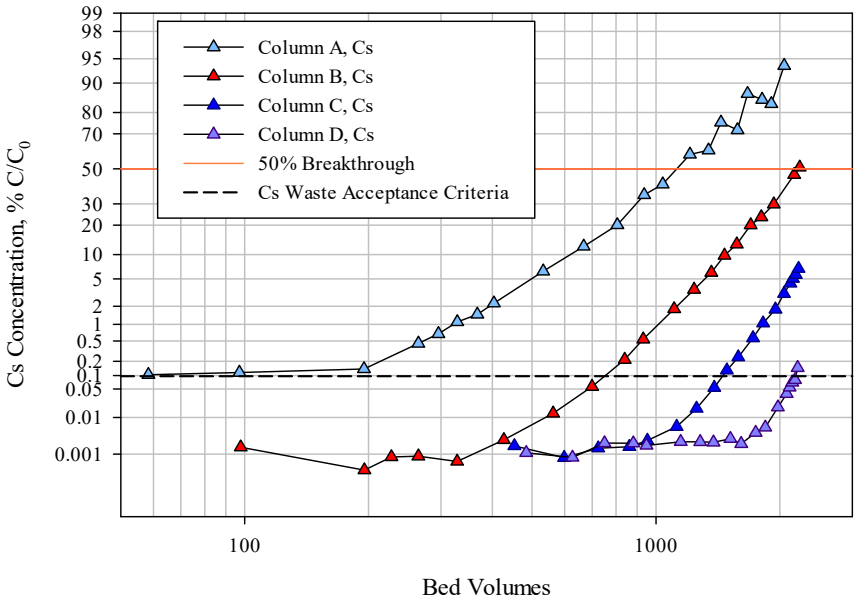

Figure 4.1. Column A, B, C, and D Cs Load Profiles of S1 Simulant at 1.4 BV/h

[9] The WAC limit was derived from the allowed curies of ^{137}Cs per mL of effluent to support railway transportation of the final treated waste form – 0.106 µCi ^{137}Cs/mL effluent. At a nominal WARM supernate feed concentration of 110 µCi ^{137}Cs/mL, the WAC limit was determined to be 0.096% C/C_0.

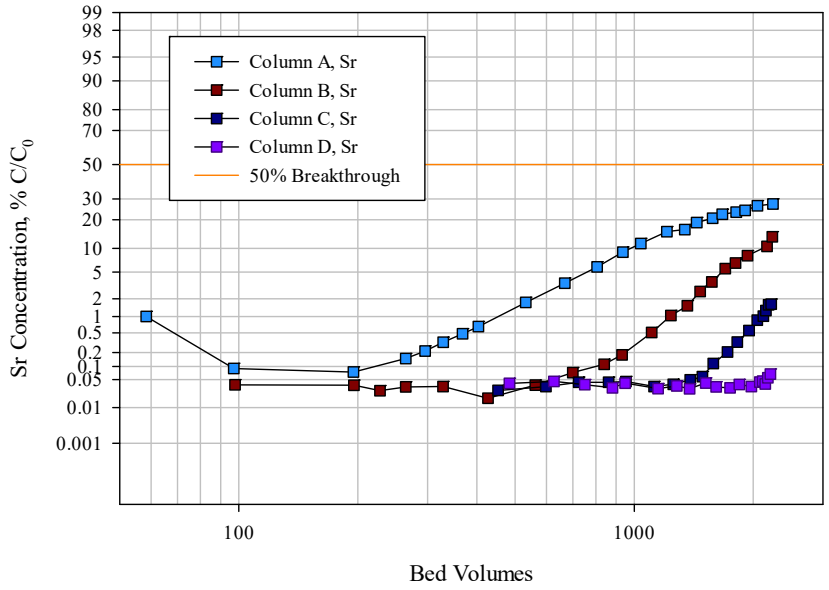

Figure 4.2. Column A, B, C, and D Sr Load Profiles of S1 Simulant at 1.4 BV/h

Figure 4.3 compares the Cs and Sr breakthroughs from the first two columns (A and B) in the IX system. Displaying the data this way gives indication of the additional capacity seen by CST for Sr over Cs. The separation between the Cs and Sr curves widens at higher BVs, with the change in slope for Sr decreasing. This behavior might suggest a slowing in the Sr loading kinetics but may also just be an experimental anomaly. A flatter Sr gradient suggests CST shows a slower mass transfer efficiency for Sr but a higher functional capacity and selectivity relative to Cs. At the conclusion of testing, column A reached an effective Cs breakthrough of 97.3% C/C_0 for Cs and only 27.4% C/C_0 for Sr. Additionally, column B concluded testing at 50.8% C/C_0 for Cs and 13.5% C/C_0 for Sr. Table 4.1 summarizes all four column breakthrough points at the conclusion of testing.

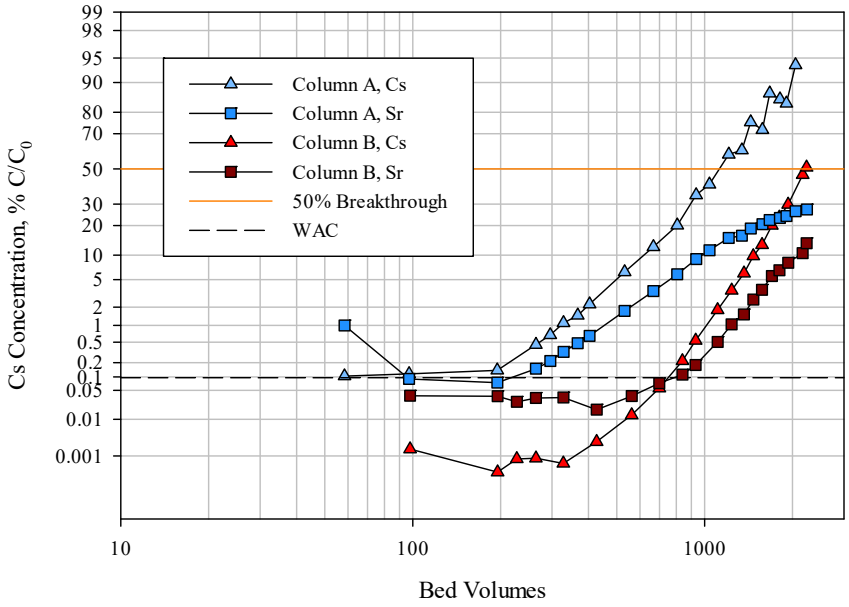

Figure 4.3. Columns A and B Cs and Sr Load Profile Comparison

Table 4.1. Final Cs and Sr Breakthrough Points

Column	Final Cs % C/C_0	Final Sr % C/C_0
A	97.25	27.39
B	50.80	13.48
C	6.55	1.63
D	0.10	0.07

Both the Sr and Cs breakthrough curves were modeled by the error function (erf) model originally described by Hougen and Marshall (1947) and Klinkenberg (1948), expressed in Eq. (4.1):

$$\frac{C}{C_0} = \frac{1}{2}\left(1 + \text{erf}\left(\sqrt{k_1 t} - \sqrt{k_2 z}\right)\right) \quad (4.1)$$

where:

k_1 and k_2 = parameters dependent on column conditions and IX media performance
t = time (or BVs processed)
z = column length

This formulation was applied to generate fits for both Cs and Sr breakthrough data for columns A, B, C, and D, as presented in Figure 4.4 through Figure 4.7. Note that Sr breakthrough results for column D are not included because Sr loading was insufficient to produce a meaningful breakthrough curve. The k1 and k2 values represent the combined effects of mass transfer coefficient, particle size, bed porosity, and residence time. Given that all columns (A-D) should have the same effective mass transfer and capacity, a single k1 value was determined by minimizing the overall error across all four columns rather than fitting each column independently. The k2 parameter was similarly solved through a global error minimization but was scaled appropriately for each successive column to capture differences in residence time. This unified fitting approach enables a more meaningful comparison between observed breakthrough behavior and the expected system performance.

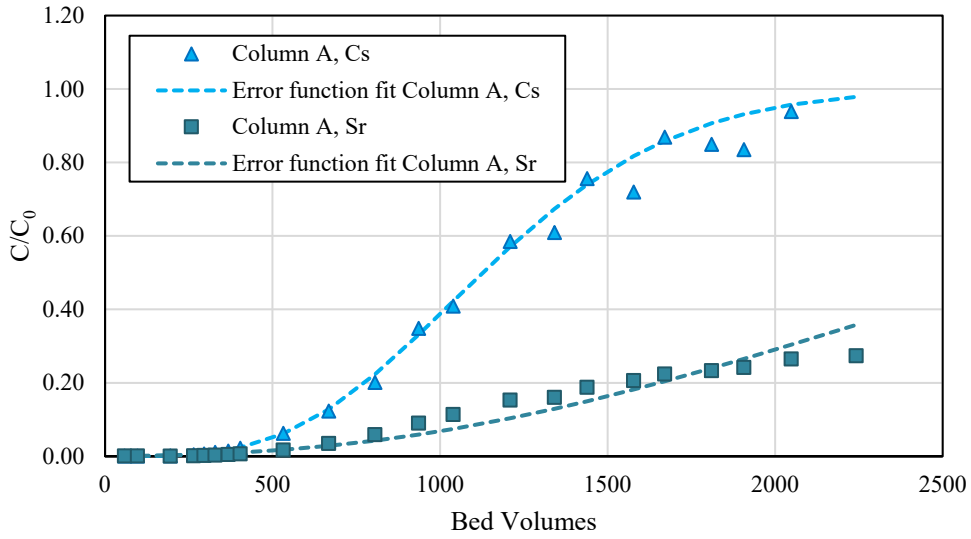

Figure 4.4. S1 Simulant Column A Cs and Sr Breakthroughs with Error Function Fits

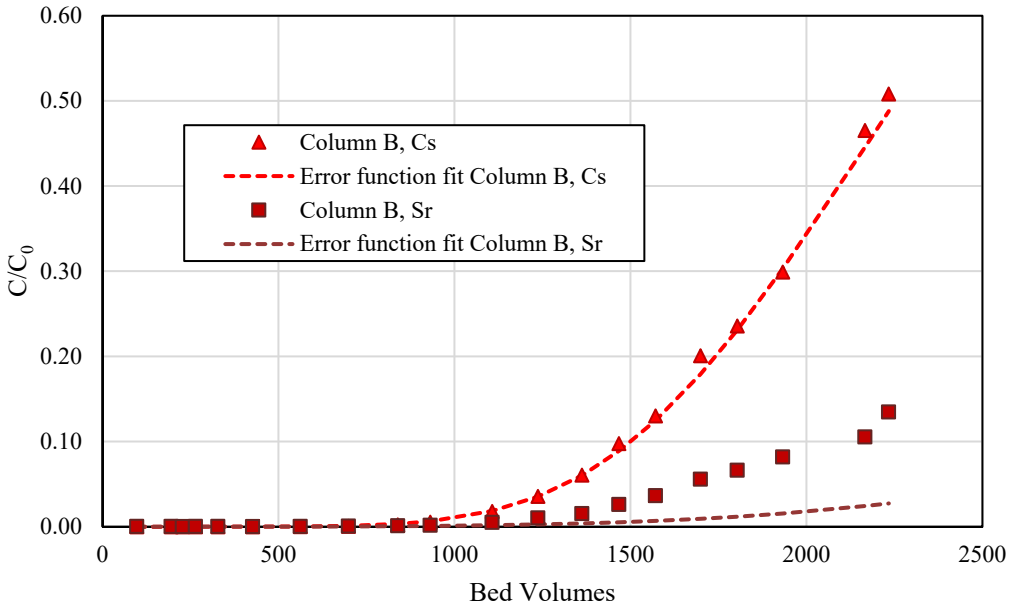

Figure 4.5. S1 Simulant Column B Cs and Sr Breakthroughs with Error Function Fits

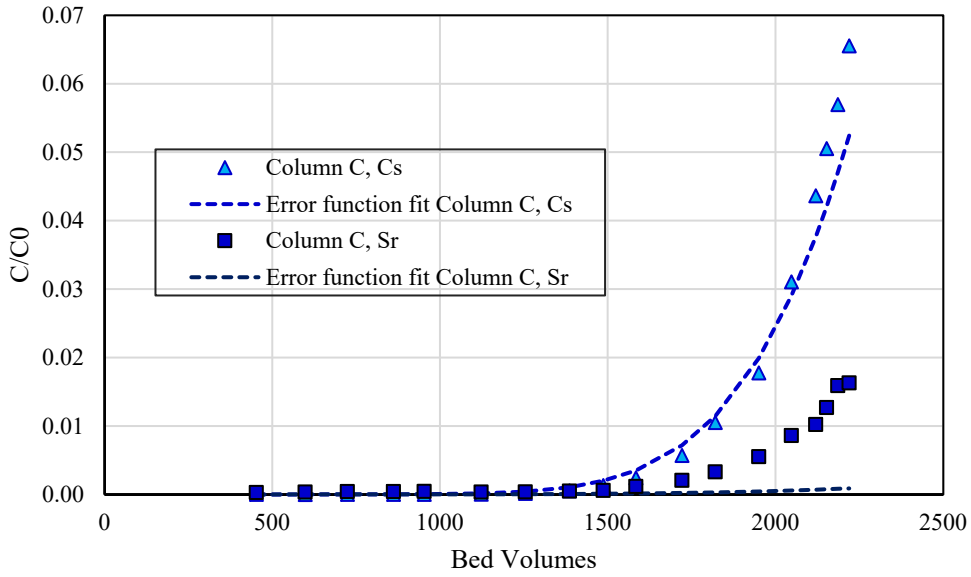

Figure 4.6. S1 Simulant Column C Cs and Sr Breakthroughs with Error Function Fits

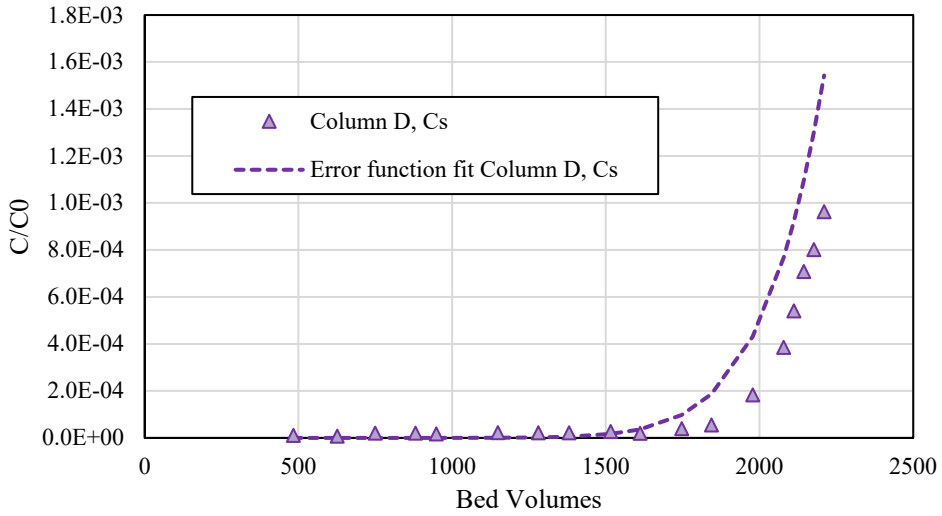

Figure 4.7. S1 Simulant Column D Cs Breakthrough with Error Function Fit

A consistent observation across the dataset is that Sr exhibits earlier-than-predicted breakthrough in columns B and C relative to the model. The underlying cause of this deviation is not yet understood, and additional testing would be required to identify the controlling mechanisms. The nature of the data suggests that the second and third columns may have slightly reduced effective capacity for Sr relative to the lead column. Additionally, a comparison of the fitted k1 values for Cs and Sr indicates that Sr loading proceeds at 25% the kinetic rate of Cs. This reduced rate may be partially attributed to the larger effective size of Sr-bearing species in solution [e.g., $Sr(OH)_2$, $Sr(NO_3)_2$, $Sr(NO_2)_2$)] compared to the monatomic Cs^+ ion. The 50% Cs and Sr breakthrough values from the error function fit, along with the k1 and k2 values for columns A, B, C, and D, are presented in Table 4.2. Note: The values in Table 4.2 are reported as $1/K_1$ and K_2, a conversion adopted to simplify the determination of the 50% breakthrough point, which is given by the product of $1/K_1$ and K_2.

Table 4.2. ERF 1/k1, k2, and 50% Breakthrough Projections

	1/k1		k2		50% Breakthrough from ERF (BVs)	
Column	Cs	Sr	Cs	Sr	Cs	Sr
A	92.5	387.0	12.2	7.1	1127	2750
B	92.5	387.0	24.4	14.0	2254	5499
C	92.5	387.0	36.5	21.1	3380	8249
D	92.5	387.0	48.7	28.1	4507	10998

A comparison of the 50% breakthrough values indicates that CST exhibits an approximate 2.44:1 capacity ratio of Sr to Cs under the conditions tested. This outcome aligns closely with the work of Campbell et al. (2020), who reported a similar Sr:Cs loading ratio of 2.29:1 based on batch isotherm measurements. The trend is further supported by the multicomponent IX modeling results of Zheng et al. (1997), which estimated CST capacities of 1.20 mmol Sr/g CST and 0.58 mmol Cs/g CST, corresponding to a 2.2:1 Sr:Cs capacity ratio. Collectively, these independent lines of evidence demonstrate that CST consistently favors Sr over Cs, yielding roughly double – or more – the effective loading for Sr across both experimental and model-based evaluations.

The railway WAC limit Cs breakthrough values were interpolated for each column by curve-fitting the BVs processed as a function of the log % C/C_0 values (Figure 4.8). The curves were fitted to a second-order polynomial function ($R^2 \geq 0.99$) and the WAC limit breakthrough values were then calculated, resulting in the following:

- Column A: 186 BVs
- Column B: 753 BVs
- Column C: 1467 BVs
- Column D: 2176 BVs

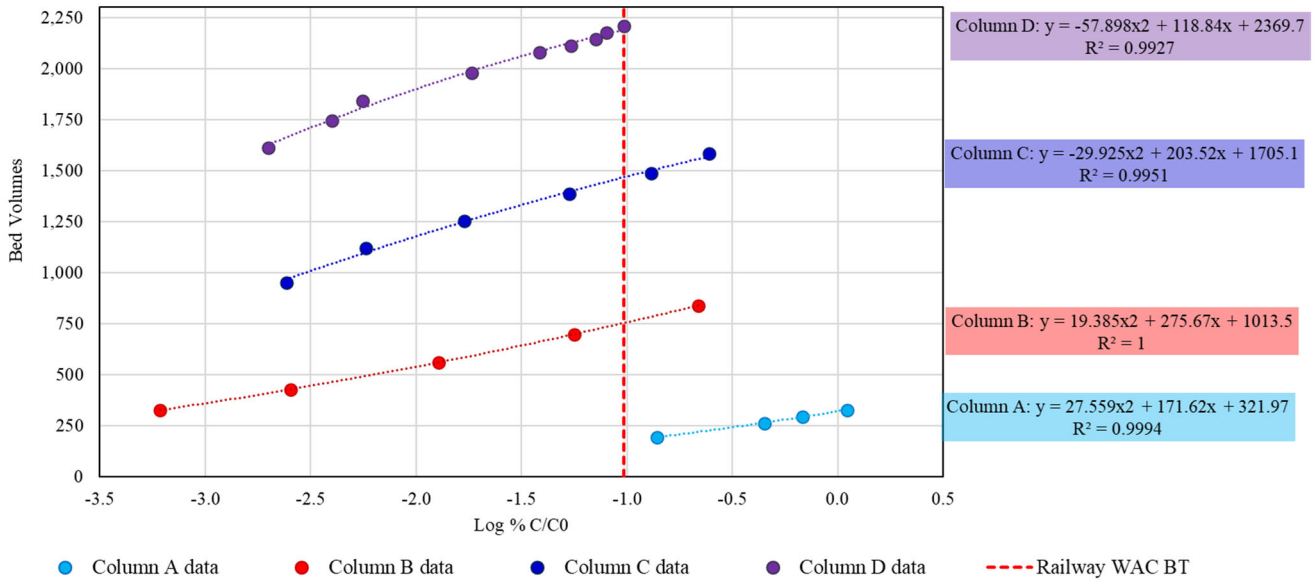

Figure 4.8. Curve Fits to Interpolate WAC Limit Breakthrough Values from S1 Columns A-D

4.1.2 Processing Projections for WARM

The influence of flowrate on the BVs processed before reaching the WAC limit was evaluated by treating different combinations of the test columns as single, integrated systems. The flowrates through four system configurations were examined:

1. Column A alone
2. Columns A and B combined
3. Columns A, B, and C combined
4. Columns A, B, C, and D combined

Under this framework, a given superficial velocity corresponds to different effective flowrates when expressed in BV/h. For example, columns A and B together operate at half the BV/h of the A system alone, since the same volumetric flow is distributed across twice the CST BV. This trend continues as additional columns are added: The effective flowrate decreases for the A-C system and decreases further for the A-D system.

To enable direct comparison of performance, the BVs processed to reach the Cs WAC limit were normalized to each redefined system in terms of system volumes (SVs). Table 4.3 summarizes the CST BV (now shown in terms of SVs), superficial velocity, resulting system flowrate in BV/h, equivalent flowrate in gallons per minute (gpm) for the WARM configuration (assuming a 157-gallon CST bed), and the normalized SVs achieved at the WAC limit.

Table 4.3. Column System Performance

System ID	CST SV (mL)	Superficial Velocity (cm/min)	Flowrate (SV/h)	Equiv. WARM (gpm)[(a)]	Normalized SVs to WAC Limit
Column A	6	0.079	1.40	14.7	175
Columns A/B	12	0.079	0.70	7.4	375
Columns A/B/C	18	0.079	0.47	4.9	490
Columns A/B/C/D	24	0.079	0.35	3.6	544

(a) Assumes a CST column volume of 157 gallons.

The normalized breakthrough profiles plotted as a function of SVs in Figure 4.9 illustrate how decreasing the flowrate – implemented by increasing the number of columns combined into a single system – directly improves CST column performance. As seen from the interface of the SVs with the dashed WAC line, measurable impacts in the mass transfer zone cause divergence among the four systems, with lower flowrates allowing more gallons to be processed before reaching the WAC due to longer residence times. A fit to the data between 3 and 8 gpm was conducted to interpolate performance at processing conditions needed for WARM flowsheet planning. Figure 4.10 displays this relationship and emphasizes that even moderate changes in flowrate can have a substantial impact on total gallons processed before the Cs waste criteria is met.

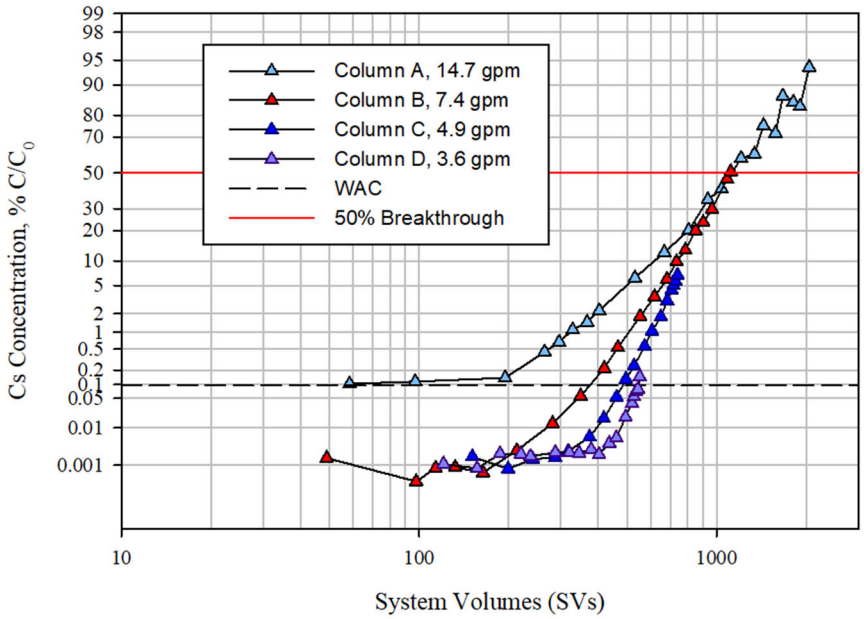

Figure 4.9. Normlized Flowrate Breakthrough for WARM Projections

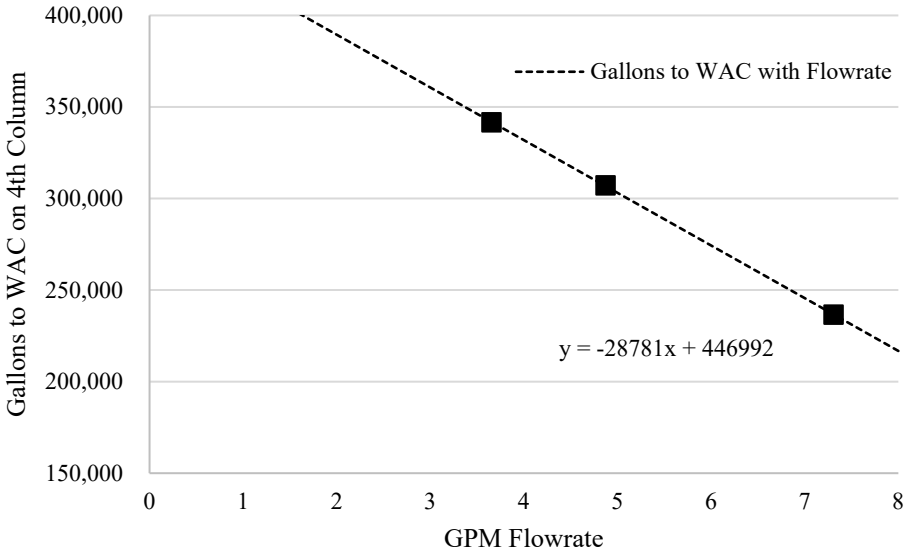

Figure 4.10. WARM Flowrate to WAC Projections

4.1.3 Cs and Sr Distribution on CST Beds

Figure 4.11 and Figure 4.12 show plots of the measured ^{137}Cs and ^{85}Sr net peak count rate as a function of position in a single "effective" column that is the combined length of the four individual columns. There was detection of ^{137}Cs in all the scans above the background condition, whereas ^{85}Sr was only detected above background on the lead column. Activity downticks for both Cs and Sr were detected at the very top and bottom of each column. These downticks are likely attributable to the scanner approaching or leaving the realm of the CST bed and do not represent a decline in activity. The Cs mass transfer zone can be estimated from 1 cm (the top of column A) through at least 11.5 cm (into the top of column 4) assuming that the top of column A from 0 to 3 cm deep represents the fully loaded CST. No Sr activity above background was measured for column B, and no detectable Sr was observed for columns C or D. This lack of measurable signal may be due to the relatively short half-life of ^{85}Sr (65 days) combined with the very low total Sr loading onto these columns, both of which would reduce detectable activity to below instrument limits.

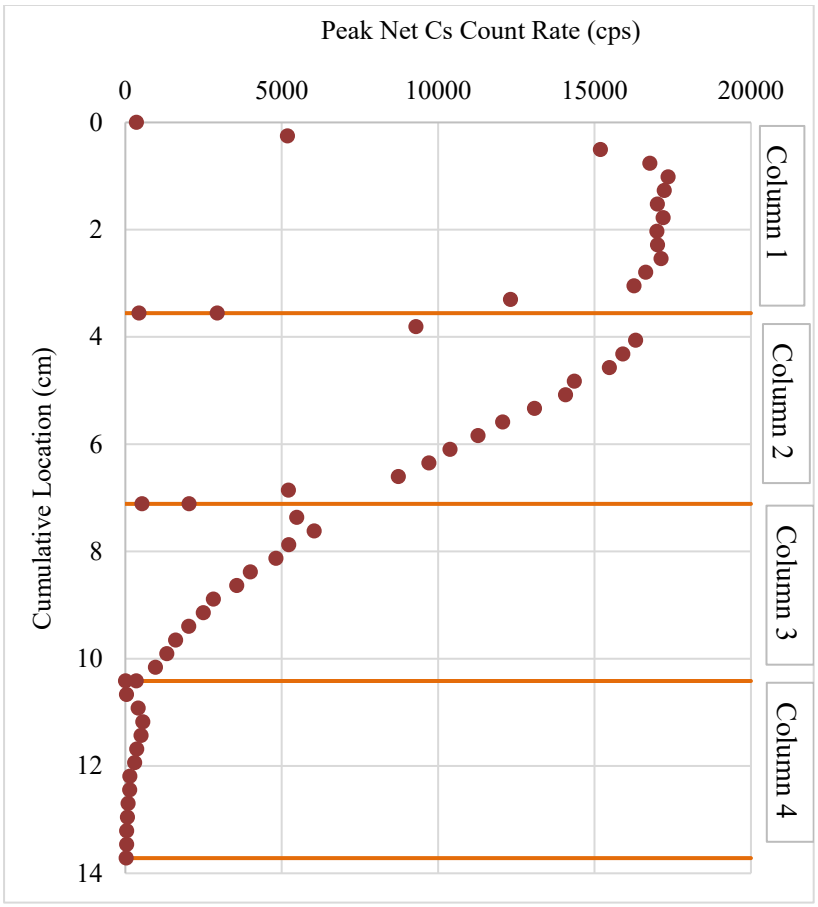

Figure 4.11. ^{137}Cs Data for the Orange Columns 1-4 Plotted as a Single Effective Column

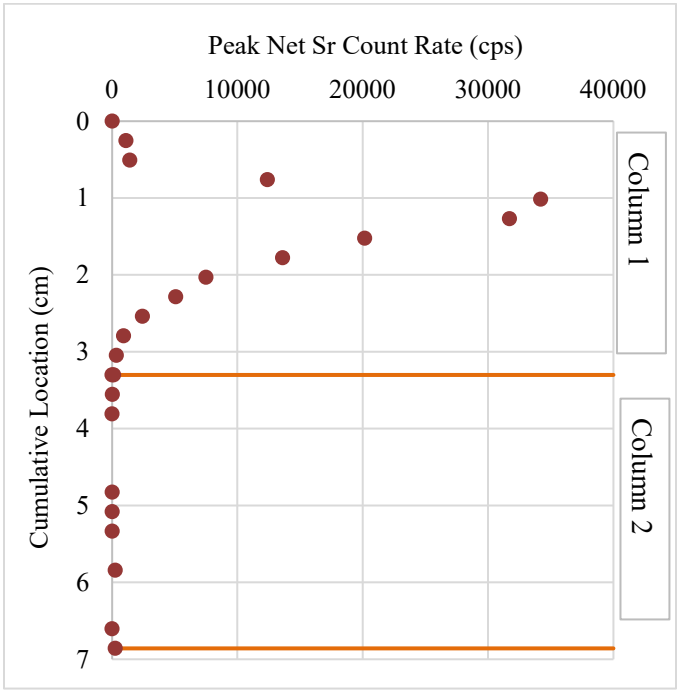

Figure 4.12. ^{137}Cs Data for the Orange Columns 1-4 Plotted as a Single Effective Column

4.1.4 Feed Displacement and Drying Impacts on Subsequent Loading

Following the conclusion of the S1 simulant loading, each column was flushed with 12 BVs of 0.1 M NaOH followed by 12 BVs of DI water to displace the feed and condition the beds for drying. The columns were then dried with compressed air until the CST became free-flowing (~72 h). Once dry, the columns were removed and gamma-scanned (see Section 4.1.3) and then reinstalled on the IX manifold. To determine whether drying affected performance, an additional 100 BVs of S1 simulant were processed through the columns, with samples collected semi-daily to determine any change in post-drying Cs capacity. As shown in Figure 4.13, no discernible loss in capacity was observed following the drying process, with the post-drying breakthrough overlaying closely with the corresponding pre-drying data. This suggests the drying processing does not measurably degrade CST Cs capacity or mass transfer performance.

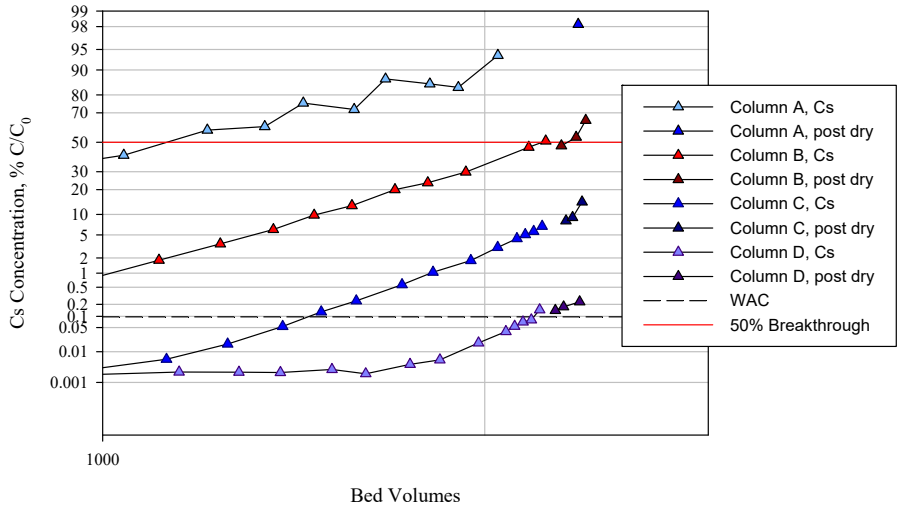

Figure 4.13. Columns A through D Cs Load Profile Comparison Pre and Post Column Drying

4.2 S1 through S5 Cs Batch Contact Results

This section provides the K_d and isotherm curves for S1 through S5 WARM simulants at test temperatures of 20 and 35 °C.

4.2.1 K_d and Isotherm Results

Figure 4.14 and Figure 4.15 show the K_d dependence on Cs concentration for all five simulants at target temperatures of 20 and 35 °C, respectively. The K_d decreased with increasing temperature, consistent with previous batch contact testing with tank waste supernate (Westesen et al. 2022, 2023, 2024, 2025; Fiskum et al. 2021). Additionally, the feed matrix had a pronounced influence on Cs capacity, with the S3 simulant – characterized by the lowest concentrations of Na^+, NO_3^-, NO_2^-, and K^+ – showing markedly better performance than the other four simulants. Table 4.4 summarizes the key cation and anion concentrations in each simulant that are known to influence Cs removal.

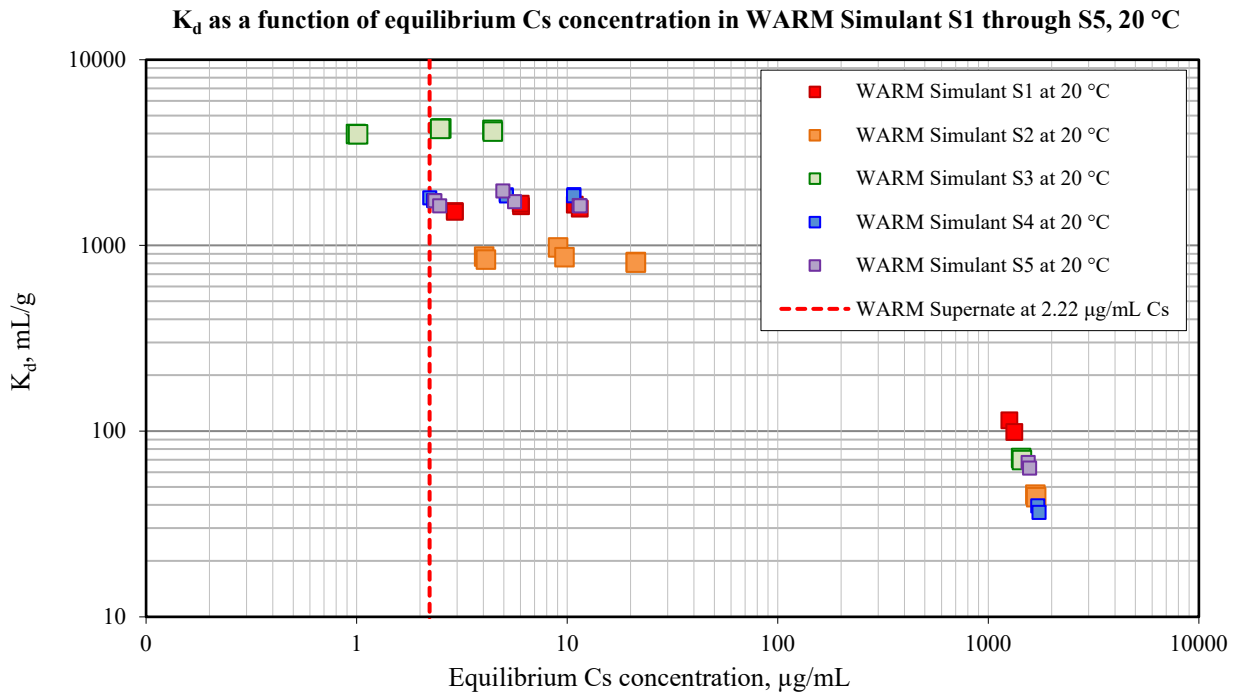

Figure 4.14. Cs K_d vs. Cs Concentration, WARM Simulants S1-S5, 20 °C

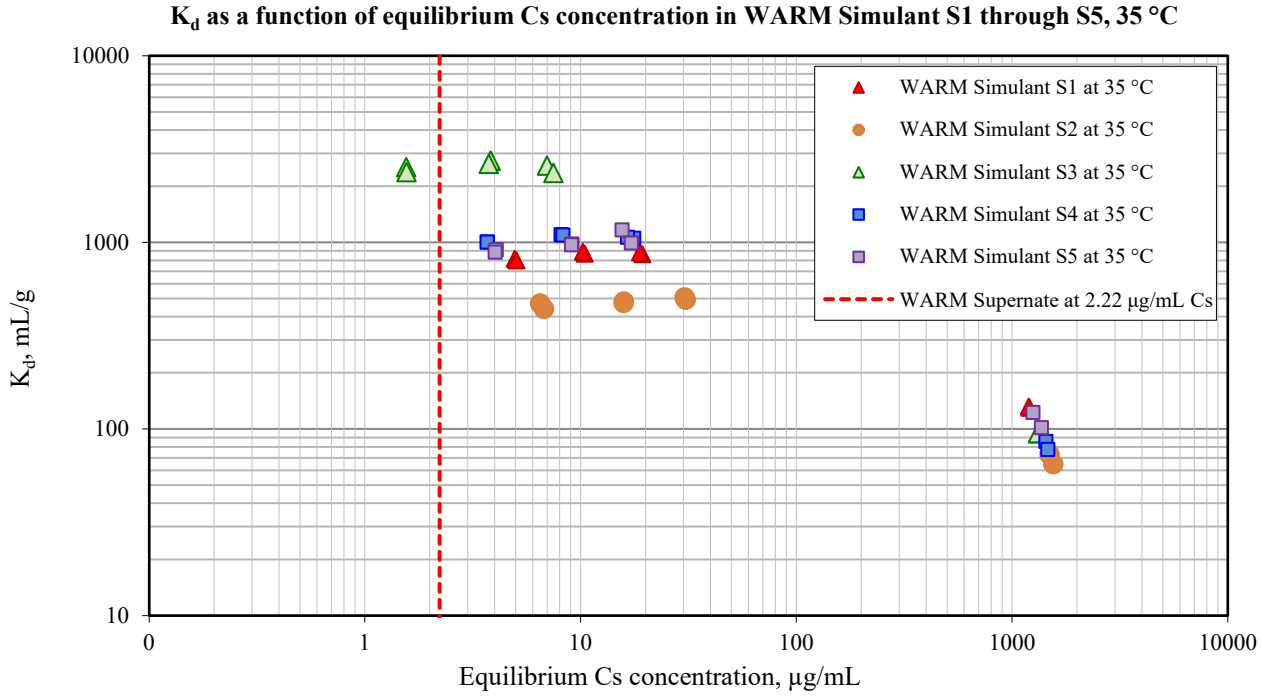

Figure 4.15. Cs K_d vs. Cs Concentration, WARM Simulants S1-S5, 35 °C

Table 4.4. S1 through S5 Key Cation and Anion Concentrations

Analyte	S1	S2	S3	S4	S5
Na^+	5.63	5.04	1.90	3.56	4.11
NO_3^-	1.62	3.64	0.83	1.52	2.10
NO_2^-	1.13	0.25	0.22	0.41	0.36
OH^-	2.10	0.67	0.41	1.08	1.09
K^+	0.04	0.01	0.01	0.02	0.01

Equilibrium loading onto CST, described as Q (mmoles Cs/g dry CST), was determined for each simulant and testing condition using the Freundlich/Langmuir hybrid equilibrium model as given in Eq. (4.2) (Hamm et al. 2002):

$$Q = \frac{\alpha_I \times [Cs]}{(\beta + [Cs])} \tag{4.2}$$

where:

[Cs] = equilibrium Cs concentration, mmoles/mL or M
Q = equilibrium Cs loading on the CST, mmole Cs per g CST
α_i = isotherm parameter constant (mmoles/g), equivalent to total capacity in the matrix
β = isotherm parameter constant (mmoles/mL or M), selectivity coefficient, dependent on matrix and temperature; the larger the value, the less selective the CST is for Cs (Hamm et al. 2002)

Table 4.5 presents the K_d and Q values for each simulant and test temperature at its corresponding initial Cs concentration. The results demonstrate a broad range of performance across the five simulant matrices, indicating that matrix composition has a substantial influence on Cs removal behavior. To better compare their performances, a model developed by Robb (2025), shown in Eq. (4.3), was used to model K_d behavior for the 20 °C temperature with the variable matrix concentrations. One interesting example of this is the comparison between S1 and S2. Despite the higher sodium and potassium concentrations, S1 has nearly double the capacity as S2 due to the changes in nitrate and hydroxide.

Table 4.5. K_d and Q Summary for S1-S5 Batch Contacts

Simulant	Temperature (°C)	K_d (mL/g)	Q (mmoles/g)
S1 2.77E-05 M Cs	20	1659	0.046
	35	908	0.025
S2 6.16E-06 M Cs	20	948	0.006
	35	427	0.003
S3 5.13E-06 M Cs	20	3875	0.020
	35	2407	0.012
S4 9.24E-06 M Cs	20	1857	0.017
	35	1076	0.010
S5 8.72E-06 M Cs	20	1786	0.016
	35	1002	0.009

$$K_d = (2300 - 321[NO_3^-] + 353([OH^-] - 1) + 1055[CO_3^{-2}]) * {}^{c}/_{2} * (1 + EXP(-[K^+] * (2.633 + 4.04[NaNO_3] + 0.436[OH^-] - 4.3[CO_3^{-2}]))) \quad (4.3)$$

where c is a constant that was calculated by minimizing the error between the calculated and experimental K_d values. To enable direct comparison of loading behavior across simulants, all matrices were first normalized to an equivalent sodium concentration of 5.6 M and then adjusted back to the original Na concentration. A summary of the results is presented in Table 4.6 along with a parity plot of the modeled K_d values, with experimental K_d values displayed in Figure 4.16. This analysis makes it clear that the differences in capacity observed in the batch contact tests arise solely from variations in matrix composition, despite the differing initial Cs concentrations.

Table 4.6. K_d and Q Summary for S1-S5 Batch Contacts

Simulant	K_d (mL/g)	K_d at 5.6 M Na (mL/g)	Modeled K_d at 5.6 M Na (mL/g)	Modeled K_d at original Na (mL/g)
S1	1659	1667	1639	1632
S2	948	853	750	834
S3	3875	1312	1280	3779
S4	1857	1181	1308	2057
S5	1786	1309	1223	1669

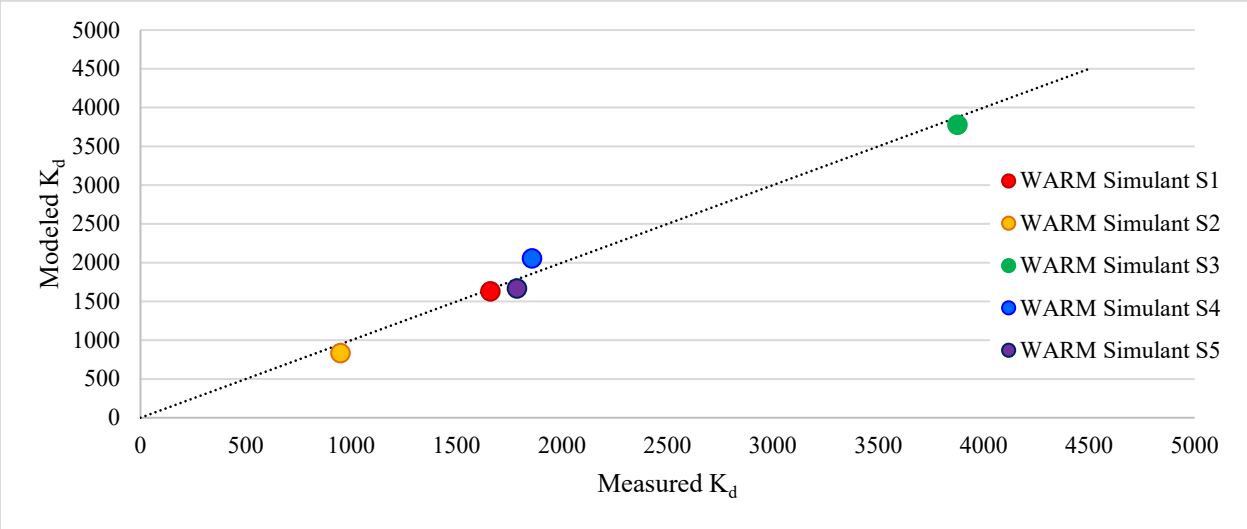

Figure 4.16. Measured and Modeled K_d Values for S1-S5 Simulant Batch Contacts

4.3 Phosphate Precipitation Determination

Phosphate precipitation behavior in the S4 simulant was evaluated to determine the extent to which PO_4^{3-} remains soluble under three test conditions and to identify any potential for precipitation and column plugging. The S4 simulant represents one of the higher-phosphate matrix compositions of the five available simulants and therefore provides a conservative basis for assessing precipitation tendencies in the broader simulant set.

During preparation of the 0.2 M PO_4 feed, after reagent addition and cooling to room temperature, the solution resulted in a rapid formation of a fine white precipitate, characteristic of a sodium-phosphate or mixed-metal phosphate solid phase. This precipitate was removed by filtration through a 0.45-µm membrane prior to subsampling the clarified supernate for initial composition verification by IC, ICP-OES, and carbon analysis. Analytical results showed that the intended 0.2 M PO_4 target had decreased to 0.08 M in solution, indicating that the S4 matrix exhibits a maximum phosphate solubility of approximately 0.1 M under these conditions.

The three feed samples (0.06, 0.1 and 0.08 M PO_4) were transferred to the temperature-controlled chamber set to 16 °C and held for 72 h to assess precipitation. After the 72 h hold time, all solutions were removed, and solids precipitation was assessed. The 0.1 and 0.08 M PO_4 feeds showed significant precipitation in the contacted solutions. Solids were filtered out (Figure 4.17) and sent for XRD analysis. The resulting supernate solutions were filtered through a 0.45-µm membrane prior to subsampling the clarified supernate for final composition assessment by IC, ICP-OES, and carbon analysis. Table 4.7summarizes the pre- and post-contact solutions along with percent precipitated. The XRD results (Figure 4.18) fit the pattern of $Na_3PO_4\,(NaOH)_{0.25}(H_2O)_{12}$ and appeared to be a pure material.

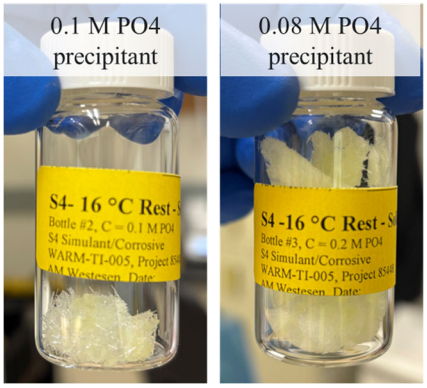

Figure 4.17. Phosphate Precipitant Collected Post Cooling of 0.1 and 0.08 M PO_4 Solutions

Table 4.7. PO_4 Precipitation Results

Bottle ID	Feed Analytical Sample ID	Initial PO_4 Concentration (M)	Actual:Target	Post Precipitation Sample ID	Final PO_4 Concentration (M)	% Precipitated
S4- 0.06 M PO4	Bottle #1-SA	0.055	0.87	Bottle #1-16-SA	0.057	2%
	Bottle #1-SB			Bottle #1-16-SB		-9%
S4-0.1 M PO4	Bottle #2-SA	0.097	0.97	Bottle #2-16-SA	0.057	42%
	Bottle #2-SB			Bottle #2-16-SB		40%
S4-0.2 M PO4	Bottle #3-SA	0.077	0.38	Bottle #3-16-SA	0.054	31%
	Bottle #3-SB			Bottle #3-16-SB		28%

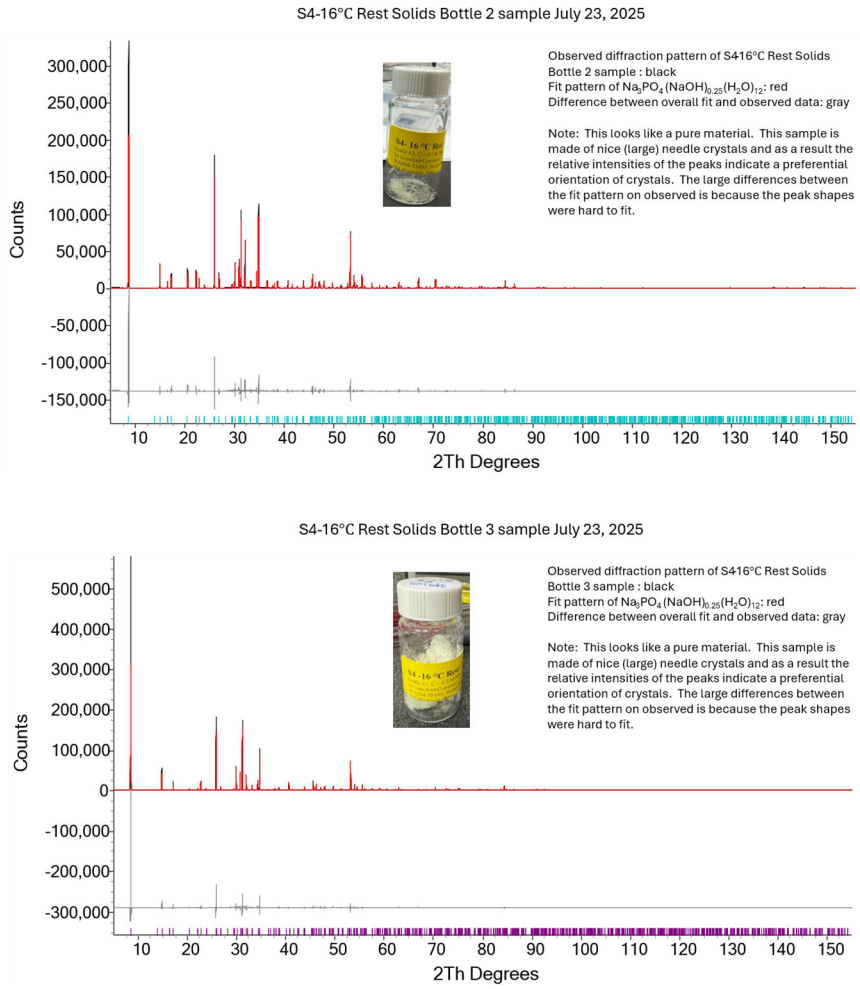

Figure 4.18. Phosphate Precipitant Collected Post Cooling of 0.1 M (top) and 0.08 M (bottom) PO_4 Solutions

Co-precipitation of other metal analytes, anions, and carbon species was also assessed but remained unchanged within analytical variability, demonstrating that the precipitation event solely affected phosphate. The batch testing results informed a subsequent evaluation of column performance. The S4 simulant, containing its native 0.06 M PO_4, was processed through a column for 1 week at 16 °C, with daily monitoring of pressure and inspection for solids accumulation on top of the CST bed. No pressure increase or observable solids buildup occurred over the duration of the test, indicating that operation under these conditions presents no concerns for WARM flowsheet planning.

4.4 Reduced Hydroxide Feed Displacement Results

The reduced-hydroxide feed-displacement evaluation was performed to determine whether lowering the free hydroxide concentration in the IX displacement solution would promote aluminum precipitation within the CST column system. Aluminum-bearing species (primarily aluminate) are known to exhibit strong solubility dependence on hydroxide concentration; therefore, reductions in caustic content could lead to solid formation during displacement or rinsing.

Batch processing of S1 simulant contacted with 0.1 M NaOH, 0.01 NaOH, DI water, and Columbia River water at 13 and 25 °C showed no significant indication of aluminum precipitation, both with and without the presence of CST. Almost all testing conditions with CST exhibited minor fine, light-colored particulate that may have been in the supernate from CST fines prior to displacement solution contact. Figure 4.19 shows an example of the solids seen in some of the contact vials. Due to the inconclusive batch results, the most aggressive condition was selected for column flowthrough operations (S1 simulant displaced with Columbia River water at 13 °C). No increase in differential pressure was detected during processing, and the CST bed surface remained free of any visible solids accumulation. These results indicate that although aluminum precipitation may be tenable under a reduced hydroxide FD, under these conditions the solids either remained sufficiently dispersed or passed through the bed without causing operational issues.

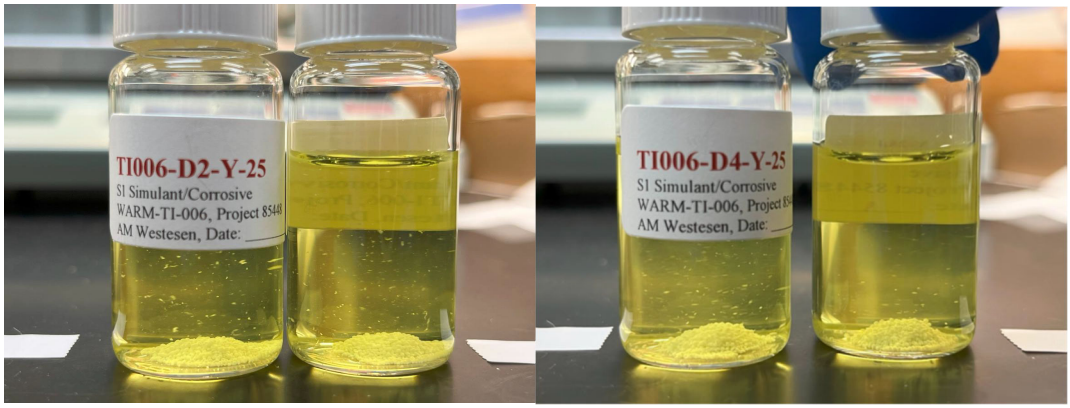

Figure 4.19. S1 Simulant with CST Contacted with 0.01 M NaOH (left) and DI Water (right)

4.5 Strontium Batch Contact Results

Table 4.8 and Table 4.9 provide the experimental results inclusive of the dry CST mass (relative to the F-factor determined at 105 °C), solution volume, solution-to-mass ratio, equilibrium Sr concentrations, distribution coefficient (K_d, mL/g CST), and molar Sr loading onto CST (Q, mmoles Sr/g CST) in the 5.5 M Na NO_3 and NO_2 matrices, respectively.

The batch distribution coefficients, K_d (mL/g) were calculated according to Eq. (4.4):

$$K_d = \frac{(C_{0i} - C_i)}{C_i} \times \frac{V}{m} \quad (4.4)$$

where C_{0i} and C_i correspond to initial and equilibrium Sr concentrations (i), respectively; V (mL) is the volume of batch contact liquid; and m (g) is the dry mass of IX material.

Table 4.8. 5.5 M Na Simulant with NO_3 Sr Batch Contact Results at 20 °C

Sample ID	Dry CST mass (g)	Simulant Vol. (mL)	Solution to Mass Ratio	Equil. Sr Conc. (M)	K_d (mL/g)	Q (mmoles Sr/g)
TI008-1A-200	0.0500	9.7967	196.1	3.46E-07	6433	2.22E-03
TI008-1A-200d	0.0493	9.7840	198.4	3.38E-07	6641	2.25E-03
TI008-1A-600	0.0505	29.3541	581.0	6.67E-07	9640	6.40E-03
TI008-1A-600d	0.0502	29.3286	584.8	7.87E-07	8159	6.38E-03
TI008-1A-1200	0.0545	60.1056	1102.2	6.06E-07	20160	1.22E-02
TI008-1A-1200d	0.0507	60.0663	1184.5	6.42E-07	20343	1.31E-02
TI008-1A-2000	0.0534	99.9529	1871.2	1.17E-06	16629	1.97E-02
TI008-1A-2000d	0.0514	99.8769	1944.5	1.42E-06	14078	2.00E-02
TI008-1B-200	0.0496	9.9186	200.0	2.29E-07	9947	2.29E-03
TI008-1B-200d	0.0502	9.8612	196.3	2.41E-07	9324	2.24E-03
TI008-1B-600	0.0502	29.6490	590.1	9.05E-07	7060	6.36E-03
TI008-1B-600d	0.0494	29.6699	600.5	--	--	--
TI008-1B-1200	0.0531	60.0923	1130.9	9.49E-07	12883	1.21E-02
TI008-1B-1200d	0.0496	60.0558	1211.0	1.14E-06	11208	1.28E-02
TI008-1B-2000	0.0487	100.0092	2055.2	2.57E-06	7360	1.87E-02
TI008-1B-2000d	0.0518	99.9795	1929.0	2.12E-06	8707	1.84E-02
TI008-1C-200	0.0507	9.7859	193.0	3.49E-07	6230	2.19E-03
TI008-1C-200d	0.0501	9.7828	195.4	3.52E-07	6296	2.21E-03
TI008-1C-600	0.0495	29.3459	592.8	--	--	--
TI008-1C-600d	0.0501	29.4192	587.7	8.18E-07	7813	6.38E-03
TI008-1C-1200	0.0462	59.9884	1297.4	1.02E-06	13708	1.38E-02
TI008-1C-1200d	0.0518	60.0180	1158.0	7.74E-07	16435	1.26E-02
TI008-1C-2000	0.0481	100.1626	2082.3	1.85E-06	11004	2.05E-02
TI008-1C-2000d	0.0509	100.1908	1968.5	1.75E-06	11091	1.95E-02
TI008-1D-200	0.0499	9.7026	195.8	2.82E-07	7892	2.23E-03
TI008-1D-200d	0.0503	9.7809	193.9	2.48E-07	9016	2.22E-03
TI008-1D-600	0.0486	29.2445	606.3	1.43E-06	4352	6.21E-03
TI008-1D-600d	0.0512	29.3938	574.4	--	--	--
TI008-1D-1200	0.0526	59.9353	1141.2	1.88E-06	6054	1.12E-02
TI008-1D-1200d	0.0524	60.0400	1144.9	--	--	--

Table 4.9. 5.5 M Na Simulant with NO_2 Sr Batch Contact Results at 20 °C

Sample ID	Dry CST mass (g)	Simulant Vol. (mL)	Solution to Mass Ratio	Equil. Sr Conc. (M)	K_d (mL/g)	Q (mmoles Sr/g)
TI008-2A-200	0.0507	29.1946	11.8081	5.89E-07	3604	1.07E-04
TI008-2A-200d	0.0494	29.0349	11.9033	5.36E-07	4130	1.09E-04
TI008-2A-600	0.0497	62.4160	35.5905	1.06E-06	5860	3.10E-04
TI008-2A-600d	0.0488	62.4807	35.7723	1.32E-06	4723	3.04E-04
TI008-2A-1200	0.0508	99.8440	72.9413	1.03E-06	12249	6.37E-04
TI008-2A-1200d	0.0510	99.8941	73.0687	9.61E-07	13182	6.42E-04
TI008-2A-2000	0.0499	148.2214	121.5859	1.63E-06	12311	1.00E-03
TI008-2A-2000d	0.0492	148.1457	121.6964	--	--	--
TI008-2B-200	0.0496	29.0184	11.5625	1.84E-07	12153	1.11E-04
TI008-2B-200d	0.0501	29.2119	11.7240	2.10E-07	10639	1.12E-04
TI008-2B-600	0.0504	61.2070	34.4567	--		
TI008-2B-600d	0.0487	62.0743	35.3722	1.50E-06	4100	2.99E-04
TI008-2B-1200	0.0487	98.7035	72.0504	1.16E-06	11157	6.30E-04
TI008-2B-1200d	0.0474	98.8568	72.3348	--		
TI008-2B-2000	0.0506	146.5859	120.1042	2.21E-06	8315	9.46E-04
TI008-2B-2000d	0.0492	147.0344	120.2307	1.95E-06	10204	9.73E-04
TI008-2C-200	0.0506	29.1438	11.7593	2.37E-07	9199	9077
TI008-2C-200d	0.0502	29.3145	11.8884	2.48E-07	8954	8954
TI008-2C-600	0.0490	62.7345	35.9536	9.99E-07	6439	6144
TI008-2C-600d	0.0496	62.7440	35.9089	1.09E-06	5850	5850
TI008-2C-1200	0.0525	99.9941	73.1446	8.53E-07	14528	14520
TI008-2C-1200d	0.0511	100.4461	73.2998	8.77E-07	14513	14513
TI008-2C-2000	0.0501	148.8251	121.8964	1.82E-06	10784	11709
TI008-2C-2000d	0.0490	149.0753	122.1173	1.62E-06	12634	12634
TI008-2D-200	0.0503	29.1616	11.9923	3.28E-07	6741	1.11E-04
TI008-2D-200d	0.0495	29.1797	12.0246	3.85E-07	5857	1.11E-04
TI008-2D-600	0.0509	62.9855	36.1292	2.29E-06	2384	2.77E-04
TI008-2D-600d	0.0506	62.8213	35.9783		--	
TI008-2D-1200	0.0501	100.0766	73.1604	1.35E-06	9100	6.17E-04
TI008-2D-1200d	0.0493	99.7481	72.9989	1.46E-06	8451	6.09E-04

The K_d values for Sr with the variable NO_3 and NO_2 feed solutions are plotted in Figure 4.20. The K_d is nearly indistinguishable from >2000 mL/g for all solution-to-mass ratios and all matrices. These results indicate the Sr concentration was not high enough to significantly load the CST and accurately deduce impacts of anion concentration (and therefore Sr complexion).

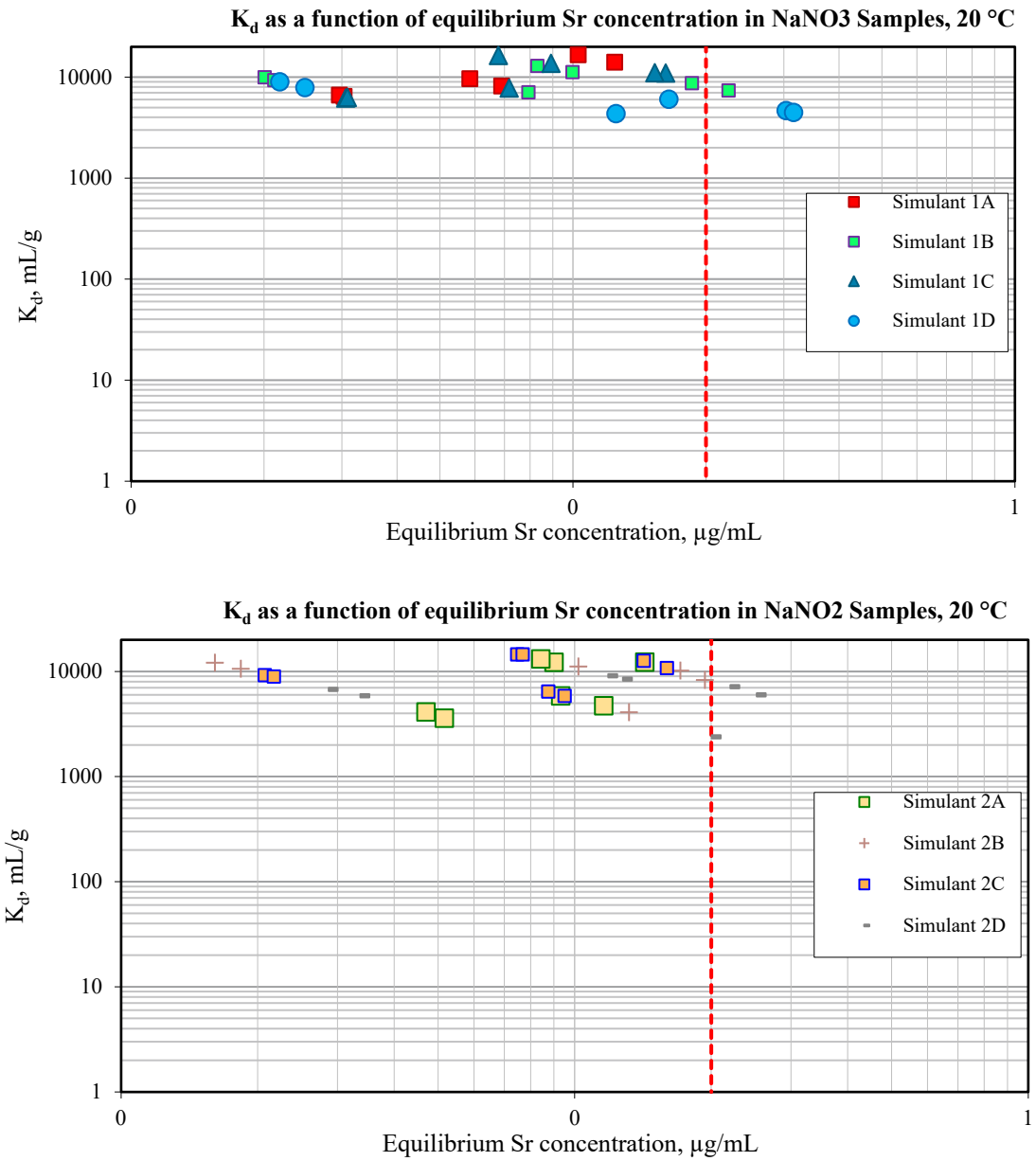

Figure 4.20. Sr K_d with CST in 5.6 M Na Simulant with NO_3 (top) and NO_2 (bottom)

Table 4.10 summarizes all the K_d values averaged from all solution to mass ratios alongside the simulant matrix. It is clear from the data that there are strong matrix dependencies on Sr sorption, with lower hydroxide concentrations favoring stronger Sr uptake in the case of the simulant 1B solution. The data is less conclusive about the impact on preference for NO_3 vs. NO_2. Additional testing is being developed to further refine these conclusions.

Table 4.10. 5.5 M Na Simulant Sr Batch Contact Results at 20 °C

Matrix ID	NaOH	$NaNO_3$	$NaNO_2$	Na_2CO_3	Kd
Simulant 1A	1	4.5	--	--	12760
Simulant 1B	4.5	1	--	--	9498
Simulant 1C	1	4	--	0.25	10368
Simulant 1D	1	2.8	--	0.85	6077
Simulant 2A	1	--	4.5	--	8008
Simulant 2B	4.5	--	1	--	9428
Simulant 2C	1	--	4	0.25	10363
Simulant 2D	1	--	2.8	0.85	6526

,

5.0 Conclusions

IX testing with CST and WARM-relevant simulants demonstrated that the planned WARM flowsheet can achieve robust Cs and Sr removal over a range of feed compositions. The work also identified key matrix dependencies and operating constraints that should be considered as WARM moves from design to operation. Specific conclusions from the testing are presented below.

5.1 Column IX Processing

A 4-column IX system using S1 simulant processed at ambient temperature showed that nominally 2200 BVs of waste can be processed before reaching the railway Cs WAC on the fourth column. Modeling and interpolation of the Cs and Sr breakthrough profiles indicated that CST provides a Sr capacity ~2.3 to 2.4 times higher than its Cs capacity, consistent with prior literature values. Sr breakthrough deviated from the predicted behavior throughout column testing and would need additional testing to assess conclusions as to why. Breakthrough data from all four columns was used to normalize an affective breakthrough behavior spanning WARM flowrates of 3 to 8 gpm to give insight into capacity reduction with increasing flowrates.

Gamma scanning of the columns confirmed that both Cs and Sr loads are distributed as expected, with the majority of loading occurring near the column inlets and progressively shifting downstream with additional BVs processed. FD and drying studies showed that the standard displacement protocol (0.1 M NaOH followed by DI water) and subsequent air drying did not measurably degrade the CST capacity or alter the Cs breakthrough behavior upon re-wetting and additional S1 processing.

5.2 S1-S5 Cs Batch Contacts

Batch contact testing with S1-S5 simulants demonstrated a wide-spread in Cs distribution coefficients and load capacities driven primarily by feed matrix effects. The data for each simulant was normalized to a 5.6 M Na concentration and compared to an anion K_d model, which indicated that differences in isotherm behavior were attributable to variations in Na, NO_3, NO_2, OH, and K. These findings emphasize the importance of matrix impacts on potential WARM processing and provide composition-specific K_d and Q inputs that can be used directly in process modeling and batch planning.

5.3 Phosphate Precipitation

The phosphate precipitation assessment with the S4 simulant established practical solubility limits and plugging risk thresholds relevant to WARM operations. Attempts to prepare 0.2 M PO_4 at 16 °C resulted in rapid formation of a fine white precipitate, and analytical results showed that the nominal 0.2 M feed actually equilibrated near ~0.08 to 0.10 M PO_4, consistent with the precipitation of a sodium phosphate. In contrast, the native 0.06 M PO_4 S4 simulant remained largely stable, and 1-week column testing at 16 °C with this feed showed no measurable pressure increase or observable solids accumulation on the CST bed. Together, these results indicate that WARM operation at or below ~0.06 M PO_4 is unlikely to be limited by phosphate-induced fouling, whereas operation at significantly higher phosphate concentrations would require additional controls on temperature, hold time, or upstream conditioning to avoid precipitation.

5.4 Reduced Hydroxide Feed Displacement

Reduced-hydroxide FD testing showed that lowering the NaOH concentration in the displacement solution can effectively displace feed without significant aluminum precipitation under the specific testing conditions. Comparisons among 0.1 M NaOH (baseline), 0.01 M NaOH, DI water, and Columbia River water at both 13 and 25 °C indicated that more dilute or non-caustic displacement chemistries can be used without adversely affecting process pressure.

5.5 Strontium Batch Contact

Sr batch contact testing with simple simulant matrices highlighted strong matrix dependencies for Sr sorption. Sr K_d values were generally >2,000 mL/g across all solution-to-mass ratios, indicating strong Sr uptake. Within the Sr concentration and speciation range tested, the data did not clearly differentiate between NO_3^- and NO_2^- effects, suggesting that additional testing at higher Sr loadings and more strongly differentiated speciation conditions will be needed to fully resolve anion and complexation impacts.

6.0 References

10 CFR 830, Subpart A, *Quality Assurance Requirements*. Code of Federal Regulations.

Abbey, L. L. 2025. *Dose Rate Scoping Assessment for Potential West Area Tank Treatment Packages using Microshield®*. Hanford Tank Waste Operations & Closure, LLC (H2C), RPP-RPT-65461, Rev. 0.. Richland, WA.

Campbell, E. L., S. K. Fiskum, T. T. Trang-Le, and R. A. Peterson. 2020. "Ion exchange of selected Group II metals and lead by crystalline silicotitanate and competition for Cs exchange sites." *Solvent Extraction and Ion Exchange*, 39 (1): 90-103. https://doi.org/10.1080/07366299.2020.1830481

DOE Order 414.1D, Quality Assurance. U.S. Department of Energy, Washington, D.C.

Fiskum, S. K., A. M. Rovira, J. R. Allred, H. A. Colburn, M. R. Smoot, A. M. Carney, T. T. Trang-Le, M. G. Cantaloub, E. C. Buck, and R. A. Peterson. 2019. *Cesium Removal from Tank Waste Simulants Using Crystalline Silicotitanate at 12% and 100% TSCR Bed Heights*. Pacific Northwest National Laboratory, PNNL-28527, Rev. 0; RPT-TCT-001, Rev. 0. Richland, WA.

Fiskum, S. K., E. L. Campbell, and T. T. Trang-Le. 2020. *Crystalline Silicotitanate Batch Contact Testing with Ba, Ca, Pb, and Sr*. Pacific Northwest National Laboratory, PNNL-30185, Rev. 0; RPT-DFTP-022, Rev. 0. Richland, WA.

Fiskum, S. K., A. M. Westesen, A. M. Carney, T. T. Trang-Le, and R. A. Peterson. 2021. *Ion Exchange Processing of AP-105 Hanford Tank Waste through Crystalline Silicotitanate in a Staged 2- then 3-Column System.* Pacific Northwest National Laboratory, PNNL-30712, Rev. 0; RPT-DFTP-025, Rev. 0. Richland, WA.

Hamm, L. L., T. Hang, D. J. McCabe, and W. D. King. 2002. *Preliminary Ion Exchange Modeling for Removal of Cesium from Hanford Waste Using Hydrous Crystalline Silicotitanate Material*. Westinghouse Savannah River Company, WSRC-TR-2001-00400; SRT-RPP-2001-00134. Aiken, SC.

Hougen, O. A., and W. R. Marshall, Jr. 1947. "Adsorption from a Fluid Stream Flowing through a Stationary Granular Bed." *Chemical Engineering Progress* 43 (4):197-208.

Klinkenberg, A. 1948. "Numerical Evaluation of Equations Describing Transient Heat and Mass Transfer in Packed Solids." *Industrial & Engineering Chemistry* 40 (10): 1992-1994.

NQA-1-2012, *Quality Assurance Requirements for Nuclear Facility Applications*. New York, NY: American Society of Mechanical Engineers.

Robb, A .M. 2025. *Sodium and Potassium Anion Effects on Cesium-137 Removal by Crystalline Silicotitanate as Applied to Simulated Liquid Hanford Tank Waste*. Georgia Tech University, Master's Thesis. Atlanta, GA.

Schonewill, P. P., L. G. El Khoury, C. A. Burns, and R. C. Daniel. 2024. *Simulant Development of Potential 200 West Area Waste Feeds*. Pacific Northwest Laboratory, PNNL-36628, Rev. 0; SWARM-RPT-001, Rev. 0. Richland, WA.

Schonewill, P.P. et. al 2026 (in-draft). *Filtration Performance of Simulated 200 West Area Waste Feeds*. Pacific Northwest Laboratory; SWARM-RPT-002, Rev. 0. Richland, WA.

Westesen, A. M., S. K. Fiskum, T. T. Trang-Le, A. M. Carney, R. A. Peterson, M. R. Landon, and K. A. Colosi. 2020. "Small to Full-Height Scale Comparisons of Cesium Ion Exchange Performance with Crystalline Silicotitanate." *Solvent Extraction and Ion Exchange* 30 (1): 104-122. https://doi.org/10.1080/07366299.2020.1831142

Westesen, A. M., E. L. Campbell, A. N. Williams, A. M. Carney, T. T. Trang-Le, and R. A. Peterson. 2022. *Reduced Temperature Cesium Removal from AP-101 Using Crystalline Silicotitanate.* Pacific Northwest National Laboratory, PNNL-32911 Rev. 0; RPT-DFTP-034, Rev. 0. Richland, WA.

Westesen, A. M., E. L. Campbell, C. Alvarez, A. M. Carney, T. T. Trang-Le, and R. A. Peterson. 2023. *Cesium Removal from 5.5 and 7.0 M Na AP-105 Using Crystalline Silicotitanate.* Pacific Northwest National Laboratory, PNNL-34395 Rev. 0; RPT-DFTP-037, Rev. 0. Richland, WA.

Westesen, A. M., A. M. Carney, E. L. Campbell, C. Alvarez, J. E. Turner, T. T. Trang-Le, and R. A. Peterson. 2024. *Ion Exchange Processing of AN-107 Hanford Tank Waste through Crystalline Silicotitanate in a Staged 2- then 3-Column System.* Pacific Northwest National Laboratory, PNNL-36241 Rev. 0; DFTP-RPT-042, Rev. 0. Richland, WA.

Westesen, A. M., A. A. Bachman, A. M. Carney, K. Bhakta, T. T. Trang-Le, and R. A. Peterson. 2025. *Ion Exchange Processing of AW-105 Hanford Tank Waste through Crystalline Silicotitanate in a Staged 2- then 3-Column System.* Pacific Northwest National Laboratory, PNNL-38102 Rev. 0; DFTP-RPT-046, Rev. 0. Richland, WA.

Zheng, Z., R. G. Anthony, and J. E. Miller. 1997. "Modeling multicomponent ion exchange equilibrium utilizing hydrous crystalline silicotitanates by a multiple interactive ion exchange site model." *Industrial & Engineering Chemistry Research* 36 (6): 2427–2434. https://doi.org/10.1021/ie960546n

Pacific Northwest National Laboratory

902 Battelle Boulevard
P.O. Box 999
Richland, WA 99354
1-888-375-PNNL (7665)

www.pnnl.gov